Master's Thesis

Scaling Properties of the Conductance of Disordered S=1 Dirac Systems

Viktor Könye

Supervisors:

Dr. József Cserti

Dr. László Oroszlány

Eötvös Loránd University
Faculty of Science
Department of Physics of Complex Systems

May 2017

Abstract

We calculate the electric conductivity of the Lieb lattice. In this system the low energy excitations are S=1 fermions, characterised by a flat band and a Dirac cone. The conductivity calculation is done in the framework of the Landauer-Bütikker approach. Employing the EQuUs code the transmission coefficient is calculated through lattice Green's functions. Investigating the effect of disorder in the sample we show that the conductivity scales with one parameter for different impurities and system sizes.

Contents

1 Introduction

1.1 Massless Dirac fermions in 2D systems

1.1.1 S=1/2

Since it's isolation in 2004 [1] and the Nobel prize in Physics in 2010 (Andre Geim and Konstantin Novoselov) graphene has a largely growing reputation. This statement is supported by the fact that the article describing the discovery of graphene [1] has been cited by more than 31000 articles, this means 7 citations per day. Graphene is a two dimensional allotrope of carbon, where the carbon atoms form a honeycomb lattice. Many of it's characteristics outrun most of the materials used today (high tensile strength, good electric and heat conduction etc.). Because of these characteristics and their possible applications (electronic devices, quantum dots, super capacitors, etc.) it is highly researched. In this work graphene will be discussed in the framework of tight binding approximation. This kind of description dates back to 1947 [**?**], where it appeared as a building block for graphite.

From the point of view of electronic transport. A very interesting property of graphene is that at low excitation energies the effective Hamiltonian can be described as pseudo-spin ($S = 1/2$) Dirac-system. This means that the dispersion relation will be a Dirac-cone with no dispersion. This causes strange behaviours in the transport properties, e.g. the Klein paradox.
it is possible to form many other lattices that have a Dirac-cone in the dispersion relation. see [2]

1.1.2 S=1

It is possible to make a pseudo-spin $S = 1$ system too, if we have three inner degrees of freedom in the unit cell. Liebről Dice-ról T3 Dirac rendszer meg-

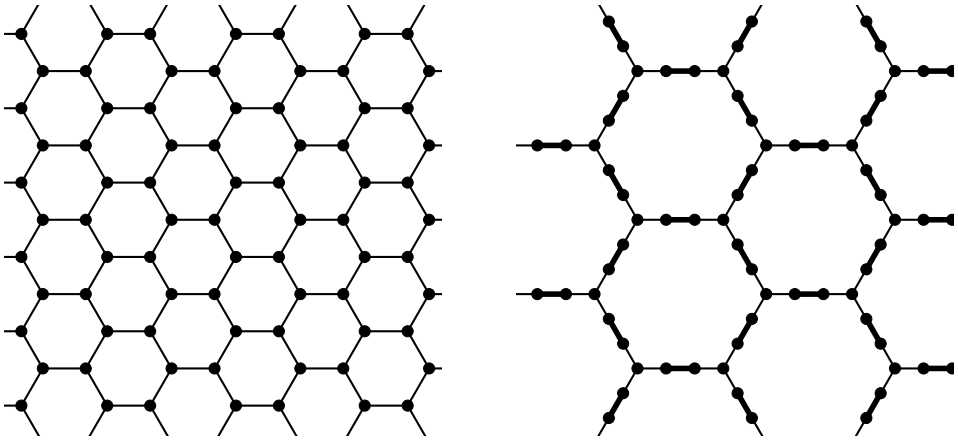

(a) Graphene (b) α-graphyne

Figure 1.1

valósíthatóság miért érdekes

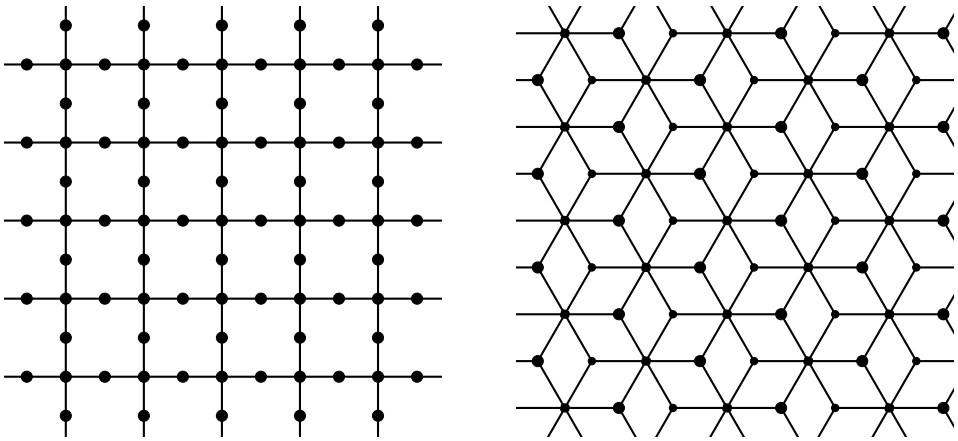

(a) Lieb lattice (b) Dice lattice

Figure 1.2

1.2 Lieb lattice

[3]

1.3 Landauer-Büttiker formalism

[4] [5] [6]

1.4 Scaling properties in disordered systems

Skálázós cikkek [7]

2 Tight-binding model of the Lieb lattice

2.1 Lieb lattice structure

The structure of the Lieb lattice can be seen on figure 2.1. The lattice plane is orthogonal to the z direction, the x and y axes are visible on the figure.

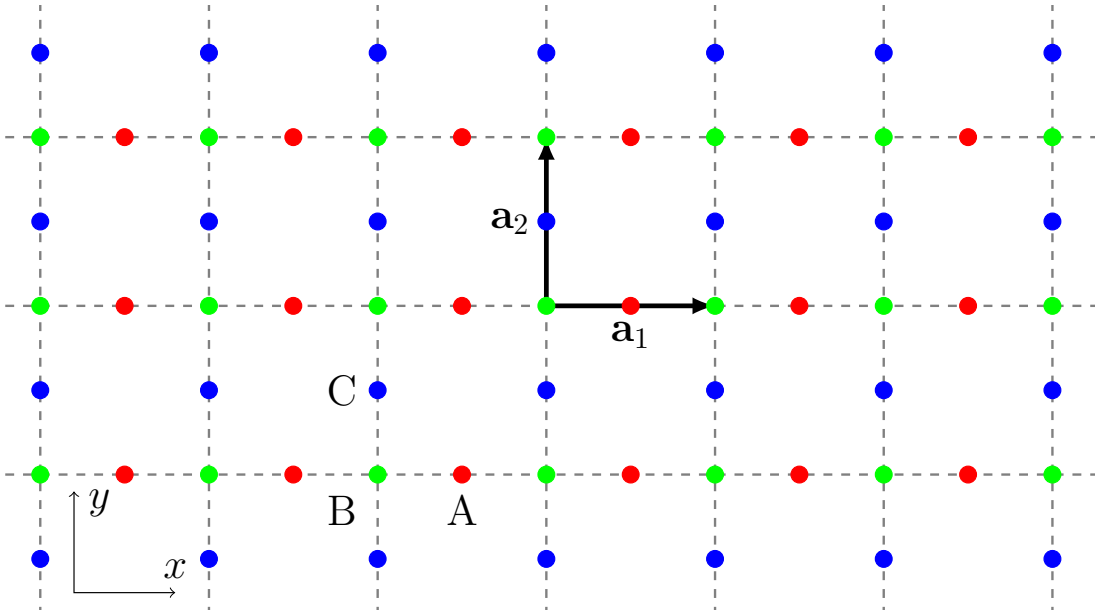

Figure 2.1: The structure of the Lieb lattice. The figure shows the primitive vectors ($\mathbf{a}_i$) of the square lattice. The three type of atoms in the unit cell are called A (red), B (green) and C (blue).

The Lieb lattice can be described as a square Bravais lattice, where in every unit cell there are three atoms. On the figure these three type of atoms in the unit cell (forming three sublattices) are called A (red), B (green) and C (blue).

The Bravais lattice is formed with the following primitive vectors:

$$\mathbf{a}_1 = \begin{pmatrix} 1 \\ 0 \end{pmatrix} , \qquad \mathbf{a}_2 = \begin{pmatrix} 0 \\ 1 \end{pmatrix} . \tag{2.1}$$

where the primitive vectors are measured in the unit of the lattice constant (a). From now on every length scale will be measured in this unit. We can define the reciprocal primitive vectors ($\mathbf{b}_i$) with the following relation:

$$\mathbf{a}_i \mathbf{b}_j = 2\pi\delta_{ij} . \tag{2.2}$$

Using the definition of the primitive vectors (2.1):

$$\mathbf{b}_1 = 2\pi \begin{pmatrix} 1 \\ 0 \end{pmatrix} , \qquad \mathbf{b}_2 = 2\pi \begin{pmatrix} 0 \\ 1 \end{pmatrix} . \tag{2.3}$$

The square Bravais lattice of the Lieb lattice and the reciprocal lattice with the Brillouin zone (BZ) are visible on figure 2.2.

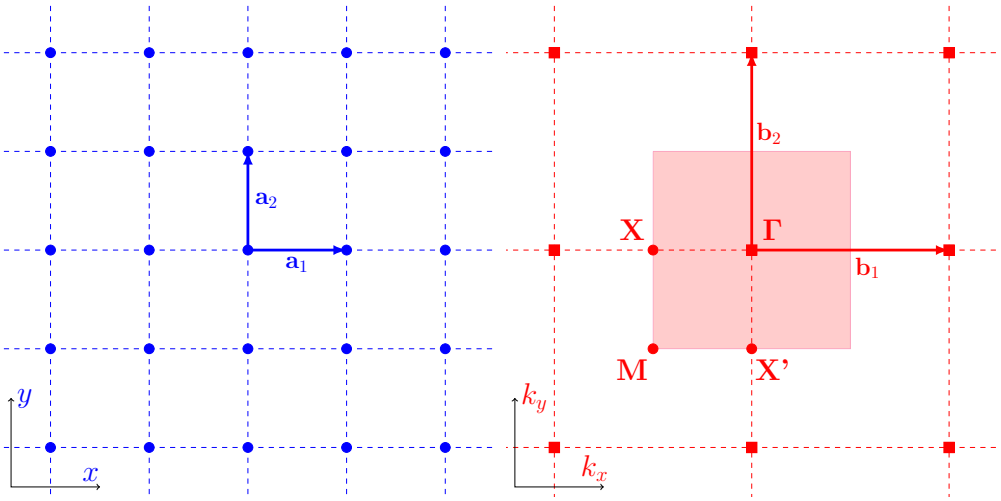

Figure 2.2: The Bravais lattice (blue) of the Lieb lattice with primitive vectors $\mathbf{a}_i$. And reciprocal lattice (red) with primitive vectors $\mathbf{b}_i$. The shaded red square is the BZ. The figure shows the high symmetry points of the BZ (Γ, X, X', M).

2.2 Hamiltonian of an infinite Lieb lattice

In this section we discuss the Hamiltonian of the Lieb lattice in the tight-binding (TB) approximation considering nearest neighbor hoppings. We can read about a general description for multiband TB system in the appendix A. For the Hamiltonian we use the followings: in the Lieb lattice there are three atoms per unit cell, on every site we consider one Wannier-state (one atomic orbital) and every nearest neighbor hopping parameter (γ) is real and has the same value for each neighbor. Since every pair contains an atom from the B sublattice we can write the second quantized Hamiltonian of this system the following way in Wannier representation:

$$H = -\sum_{\langle i,j\rangle_{ba},\sigma} \gamma(b^\dagger_{i\sigma}a_{i-j\sigma} + h.c.) - \sum_{\langle i,j\rangle_{bc},\sigma} \gamma(b^\dagger_{i\sigma}c_{i-j\sigma} + h.c.) \ , \tag{2.4}$$

where the sums goes over every nearest neighbor ($\langle i,j\rangle_{ba}$ are the unit cells where there are two neighboring A and B atoms). $a_{i\sigma}$, $b_{i\sigma}$ and $c_{i\sigma}$ are the annihilation operators of the Wannier-states in the i-th unit cell on the A, B or C sublattices having σ spin state. Applying Bloch's theorem we know that the Hamiltonian will be diagonal in the quasimomentum ($\mathbf{k}$). In systems were there are multiple atoms in a unit cell the Bloch representation is not unique [8]. For practical purposes the following representation will be used for the creation/annihilation operators of Bloch states:

$$a_{\mathbf{k}\sigma} = \frac{1}{\sqrt{N}}\sum_i \mathrm{e}^{-i\mathbf{k}\mathbf{R}_i^A} a_{i\sigma} \ , \quad b_{\mathbf{k}\sigma} = \frac{1}{\sqrt{N}}\sum_i \mathrm{e}^{-i\mathbf{k}\mathbf{R}_i^B} b_{i\sigma} \ , \quad c_{\mathbf{k}\sigma} = \frac{1}{\sqrt{N}}\sum_i \mathrm{e}^{-i\mathbf{k}\mathbf{R}_i^C} c_{i\sigma} \ , \tag{2.5}$$

where $\mathbf{R}_i^{A/B/C}$ is the vector pointing to the $A/B/C$ atom in the i-th unit cell. The normalization is chosen so to assure the normalization of the Bloch states (N is the number of unit cells). The inverse relations have the following form:

$$a_{i\sigma} = \frac{1}{\sqrt{N}}\sum_{\mathbf{k}} \mathrm{e}^{i\mathbf{k}\mathbf{R}_i^A} a_{\mathbf{k}\sigma} \ , \quad b_{i\sigma} = \frac{1}{\sqrt{N}}\sum_{\mathbf{k}} \mathrm{e}^{i\mathbf{k}\mathbf{R}_i^B} b_{\mathbf{k}\sigma} \ , \quad c_{i\sigma} = \frac{1}{\sqrt{N}}\sum_{\mathbf{k}} \mathrm{e}^{i\mathbf{k}\mathbf{R}_i^C} c_{\mathbf{k}\sigma} \ . \tag{2.6}$$

Substituting these in the Hamiltonian we get the following (to follow the calculations see appendix A where a more general case is discussed):

$$H = -\sum_{k,\sigma} 2\gamma \left[\cos\left(\frac{k_x}{2}\right) b^\dagger_{\mathbf{k}\sigma} a_{\mathbf{k}\sigma} + \cos\left(\frac{k_y}{2}\right) b^\dagger_{\mathbf{k}\sigma} c_{\mathbf{k}\sigma} + h.c. \right] . \tag{2.7}$$

Using the following definitions:

$$\mathbf{H}(\mathbf{k}) := -2\gamma \begin{pmatrix} 0 & \cos(k_x/2) & 0 \\ \cos(k_x/2) & 0 & \cos(k_y/2) \\ 0 & \cos(k_y/2) & 0 \end{pmatrix} , \quad \mathbf{a}_{\mathbf{k}\sigma} := \begin{pmatrix} a_{\mathbf{k}\sigma} \\ b_{\mathbf{k}\sigma} \\ c_{\mathbf{k}\sigma} \end{pmatrix} , \tag{2.8}$$

the Hamiltonian can be expressed as:

$$H = \sum_{k,\sigma} \mathbf{a}^\dagger_{\mathbf{k}\sigma} \mathbf{H}(\mathbf{k}) \mathbf{a}_{\mathbf{k}\sigma} = \sum_{k,\sigma} \sum_{\ell,m=1}^{3} a^{(\mathbf{k}\sigma)\dagger}_\ell H_{\ell m}(\mathbf{k}) a^{(\mathbf{k}\sigma)}_m . \tag{2.9}$$

2.2.1 Dispersion relation

The eigenvalue problem now is reduced to the eigenvalue problem of the 3×3 $\mathbf{H}(\mathbf{k})$ Hamiltonian matrix. This can be solved analytically and the dispersion relation is the following:

$$\begin{aligned} \varepsilon_0(\mathbf{k}) &= 0 , \\ \varepsilon_\pm(\mathbf{k}) &= \pm 2\gamma \sqrt{\cos^2\left(\frac{k_x}{2}\right) + \cos^2\left(\frac{k_y}{2}\right)} . \end{aligned} \tag{2.10}$$

There are 3 bands, two bands are symmetric to the zero plane, and the third is a constant zero band, also called flat band. We can see the dispersion relation of figure 2.3 evaluated on lines connecting high symmetry points and on figure 2.4 as a 3d surface plot. Since there are three atoms in every unit cell we have $3N$ electrons. Every band has $2N$ states with the spin degree of freedom. This means that the lower band is fully occupied and the flat band is half full. Also the Fermi energy is at 0. The bandwidth of the upper or lower band is $\varepsilon_\pm(\mathbf{0}) = 2\sqrt{2}\gamma$. The two symmetric bands touch each other at the corner of the BZ, at the M point.

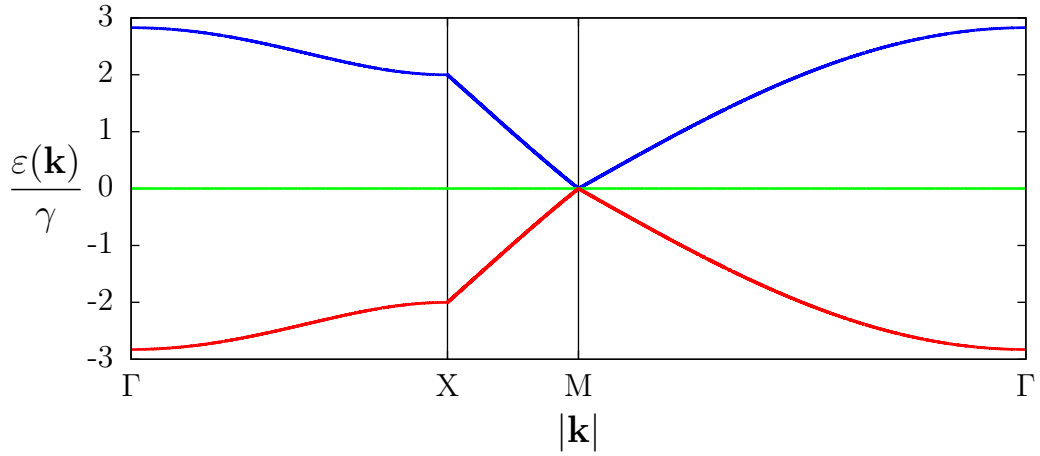

Figure 2.3: Dispersion relation of the Lieb lattice on lines connecting high symmetry points. The path shown here are straight lines going over $\Gamma - X - M - \Gamma$. The $|\mathbf{k}|$ on the x axis goes from 0 to $\sqrt{2}\pi$ until the M point and backwards until the Γ point.

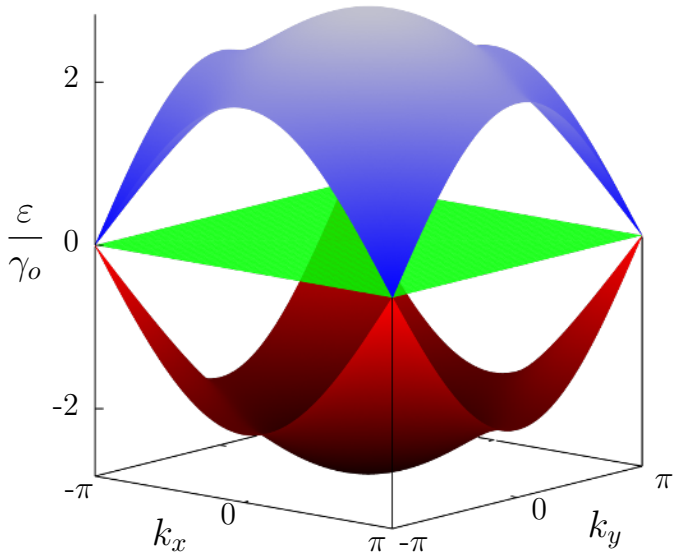

Figure 2.4: Dispersion relation of the Lieb lattice inside the BZ.

The emergence of the flat band can be understood from a symmetry point of view. The $\mathbf{H}(\mathbf{k})$ Hamiltonian matrix has a chiral symmetry. We can define a chirality operator as:

$$\boldsymbol{\mathcal{C}} = \begin{pmatrix} 1 & 0 & 0 \\ 0 & -1 & 0 \\ 0 & 0 & 1 \end{pmatrix} . \tag{2.11}$$

We can easily show that this operator anticommutes with the Hamiltonian:

$$\mathbf{H}(\mathbf{k})\boldsymbol{\mathcal{C}} + \boldsymbol{\mathcal{C}}\mathbf{H}(\mathbf{k}) = \mathbf{0} \ . \tag{2.12}$$

This has a very important consequence on the dispersion relation. If there is an eigenvector $\mathbf{v}$ with energy E then $\boldsymbol{\mathcal{C}}\mathbf{v}$ is also an eigenvector with energy $-E$. This means that the dispersion relation must be symmetric to the zero plane. And since we have a 3×3 matrix there must be three bands which can only be symmetric if one of them is a flat band. Near the M point the dispersion relation takes the form of a cone the so called Dirac cone. Let's introduce the following wavenumber:

$$\mathbf{p} = \mathbf{k} - (\pi, \pi) \ . \tag{2.13}$$

If we are close to the M point we can expand the dispersion relation as:

$$\begin{aligned} \varepsilon_{\pm}(\mathbf{p}) &= \pm 2\gamma \sqrt{\cos^2\left(\frac{p_x + \pi}{2}\right) + \cos^2\left(\frac{p_y + \pi}{2}\right)} = \\ &= \pm 2\gamma \sqrt{\sin^2\left(\frac{p_x}{2}\right) + \sin^2\left(\frac{p_y}{2}\right)} \approx \pm\gamma\sqrt{p_x^2 + p_y^2} = \pm\gamma|\mathbf{p}| \end{aligned} \tag{2.14}$$

As we can see this is a dispersionless cone, with constant group velocity. We can see this on figure 2.5. This is something similar to what we can find in graphene, but the important difference is the flat band that is also present in this case.

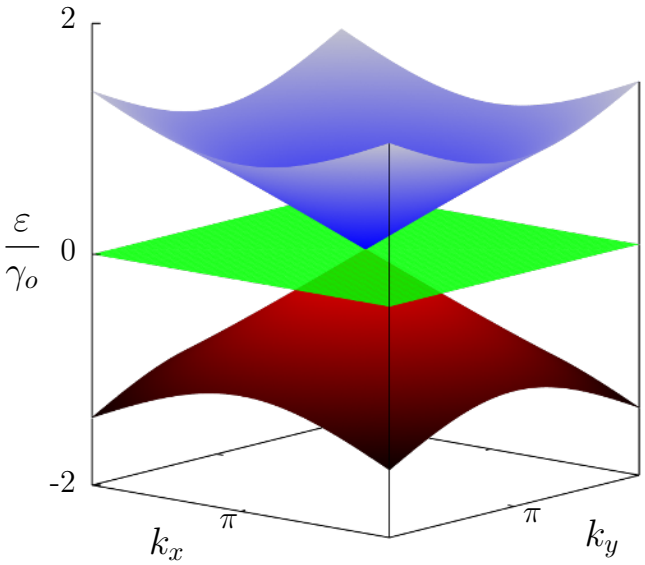

Figure 2.5: Dispersion relation of the Lieb lattice near the M point.

2.2.2 Effective $S = 1$ Dirac Hamiltonian

For low energy excitations we can approximate the (2.9) Hamiltonian to the first order of the previously defined $\mathbf{p}$ vector (2.13) as:

$$\mathbf{H}(\mathbf{p}) = \gamma \begin{pmatrix} 0 & p_x & 0 \\ p_x & 0 & p_y \\ 0 & p_y & 0 \end{pmatrix} . \tag{2.15}$$

We can express this Hamiltonian as

$$\mathbf{H}(\mathbf{p}) = \gamma \sum_{\alpha=x,y} \tilde{\mathbf{S}}_\alpha p_\alpha , \tag{2.16}$$

where the $\tilde{\mathbf{S}}_\alpha$ are defined as:

$$\tilde{\mathbf{S}}_x := \begin{pmatrix} 0 & 1 & 0 \\ 1 & 0 & 0 \\ 0 & 0 & 0 \end{pmatrix} \qquad \tilde{\mathbf{S}}_y := \begin{pmatrix} 0 & 0 & 0 \\ 0 & 0 & 1 \\ 0 & 1 & 0 \end{pmatrix} \qquad \tilde{\mathbf{S}}_z := \begin{pmatrix} 0 & 0 & -i \\ 0 & 0 & 0 \\ i & 0 & 0 \end{pmatrix} . \tag{2.17}$$

These matrices all have eigenvalues $-1, 0, 1$ and also they satisfy the following commutation relations:

$$[\tilde{\mathbf{S}}_\alpha, \tilde{\mathbf{S}}_\beta] = i \sum_\gamma \varepsilon_{\alpha\beta\gamma} \tilde{\mathbf{S}}_\gamma , \tag{2.18}$$

where $\varepsilon_{\alpha\beta\gamma}$ is the Levi-Civita symbol. This means that the introduced matrices are $S = 1$ representations of the Lie algebra of the SU(2) group. This means that they can be used to describe an $S = 1$ spin. We can also notice that these matrices are three of the eight Gell-Mann matrices. With the usual notation: $\tilde{\mathbf{S}}_x = \boldsymbol{\lambda}_1$, $\tilde{\mathbf{S}}_y = \boldsymbol{\lambda}_6$, $\tilde{\mathbf{S}}_z = \boldsymbol{\lambda}_5$. Usually this is not the representation we use for $S = 1$ spins, but the one where $\mathbf{S}_z$ is diagonal. This representation is unitarily equivalent and can be obtained the following way:

$$\mathbf{S}_i = \mathbf{U}\tilde{\mathbf{S}}_i\mathbf{U}^\dagger \qquad\qquad \mathbf{U} = \frac{1}{\sqrt{2}} \begin{pmatrix} i & 0 & 1 \\ 0 & \sqrt{2}i & 0 \\ i & 0 & -1 \end{pmatrix} . \tag{2.19}$$

With this we get the usual $S = 1$ representation:

$$\mathbf{S}_x = \frac{1}{\sqrt{2}} \begin{pmatrix} 0 & 1 & 0 \\ 1 & 0 & 1 \\ 0 & 1 & 0 \end{pmatrix} \quad \mathbf{S}_y = \frac{1}{\sqrt{2}} \begin{pmatrix} 0 & -i & 0 \\ i & 0 & -i \\ 0 & i & 0 \end{pmatrix} \quad \mathbf{S}_z = \begin{pmatrix} 1 & 0 & 0 \\ 0 & 0 & 0 \\ 0 & 0 & -1 \end{pmatrix} . \tag{2.20}$$

In this new representation obtained with $\mathbf{U}$ the low energy Hamiltonian can be expressed as:

$$\mathbf{H}(\mathbf{p}) = \gamma \sum_{\alpha=x,y} \mathbf{S}_\alpha p_\alpha \ . \tag{2.21}$$

Since this spin has nothing to do with the actual spin of the electron in the system it is usually called pseudo-spin. This Hamiltonian can be used to make a continuum model for the Lieb lattice, where $\mathbf{p}$ is thought of as a normal momentum and not as a quasi momentum. This way we obtained a Dirac-Weyl system with $S = 1$ pseudo-spin.

2.3 Hamiltonian of an infinite Lieb lattice strip

After discussing the infinite Lieb lattice we will go on with an infinite Lieb lattice strip. This means that the lattice is infinite in the x direction and has a finite W width. W will be the number of unit cells in the y direction. Depending on how we stop at the edge of the strip we can get many different boundary conditions. We can see some examples on figure 2.6.

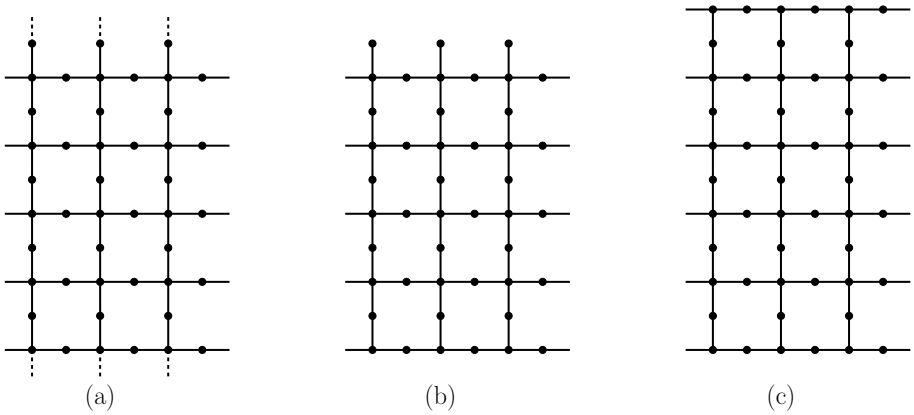

Figure 2.6: Different types of boundary conditions. Every strip is infinite in the x direction and is $W = 5$ wide. (a) periodic boundary condition (b) *hanging* boundary condition (c) *closed* boundary condition.

The basic boundary conditions we can choose are the followings. If we want to get rid of the edge of the system we can choose the periodic boundary condition as in (a). We can choose to cut the Lieb lattice with a straight line between the C and B atoms of two neighboring cells and get hanging nodes as seen in (b). Or we can cut between the B and C atoms of the same cell and get (c). Of course we don't necessarily have to cut with straight lines, but for the sake of simplicity we will only discuss those cases.

Since now there is no translational symmetry in the y direction (at least in the (b) and (c) conditions), the previous discussion used for the case of an infinite Lieb lattice can't be used. It is useful to go back to the Wannier representation and construct the one particle Hamiltonian. We can think of the Hamiltonian as a linear chain, where every node has multiple degrees of freedom. The Hamiltonian can be expressed as:

$$\hat{\mathbf{H}} = \begin{pmatrix} \mathbf{H}_0 & \mathbf{H}_1 & 0 & 0 & \dots \\ \mathbf{H}_1^\dagger & \mathbf{H}_0 & \mathbf{H}_1 & 0 & \dots \\ 0 & \mathbf{H}_1^\dagger & \mathbf{H}_0 & \mathbf{H}_1 & \dots \\ 0 & 0 & \mathbf{H}_1^\dagger & \mathbf{H}_0 & \dots \\ \vdots & \vdots & \vdots & \vdots & \ddots \end{pmatrix}, \tag{2.22}$$

where $\mathbf{H}_0$ and $\mathbf{H}_1$ are matrices. We can see on figure 2.7 how the linear chain is constructed for a simple example.

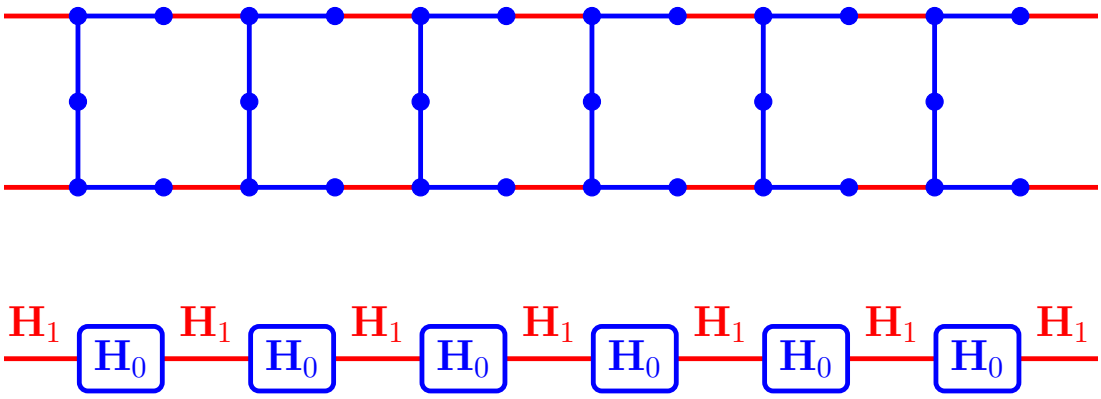

Figure 2.7: The figure shows the structure of a Lieb lattice strip (W=1 and *closed* boundary condition is used). The blue parts are described by $\mathbf{H}_0$ and the red connections between the blue parts are described by $\mathbf{H}_1$.

The $\mathbf{H}_0$ and $\mathbf{H}_1$ Hamiltonians can be constructed using the following building blocks:

$$\mathbf{h}_{00} := \begin{pmatrix} \varepsilon & -\gamma & 0 \\ -\gamma & \varepsilon & -\gamma \\ 0 & -\gamma & \varepsilon \end{pmatrix} \quad \mathbf{h}_{01} := \begin{pmatrix} 0 & 0 & 0 \\ 0 & 0 & 0 \\ 0 & -\gamma & 0 \end{pmatrix} \quad \mathbf{h}_1 := \begin{pmatrix} 0 & -\gamma & 0 \\ 0 & 0 & 0 \\ 0 & 0 & 0 \end{pmatrix} . \tag{2.23}$$

Here $\mathbf{h}_{00}$ represents the Hamiltonian inside a unit cell, $\mathbf{h}_{01}$ represents the connection between a unit cell and the unit cell above, and $\mathbf{h}_1$ represent the connection between a unit cell and the cell right to it. The γ hopping parameter and ε on-site potential can be chosen arbitrarily. We will set the energy scale using γ, so every energy is measured in the units of γ thus $\gamma = 1$. Also we can set the Fermi-energy to 0 with taking $\varepsilon = 0$. So the actual matrices that we will use in the later calculations take the following form:

$$\mathbf{h}_{00} = \begin{pmatrix} 0 & -1 & 0 \\ -1 & 0 & -1 \\ 0 & -1 & 0 \end{pmatrix} \quad \mathbf{h}_{01} = \begin{pmatrix} 0 & 0 & 0 \\ 0 & 0 & 0 \\ 0 & -1 & 0 \end{pmatrix} \quad \mathbf{h}_1 = \begin{pmatrix} 0 & -1 & 0 \\ 0 & 0 & 0 \\ 0 & 0 & 0 \end{pmatrix} . \tag{2.24}$$

With these the $\mathbf{H}_0$ and $\mathbf{H}_1$ can be constructed as:

$$\mathbf{H_0} = \begin{pmatrix} \mathbf{h}_{00} & \mathbf{h}_{01} & 0 & 0 & \dots \\ \mathbf{h}_{01}^\dagger & \mathbf{h}_{00} & \mathbf{h}_{01} & 0 & \dots \\ 0 & \mathbf{h}_{01}^\dagger & \mathbf{h}_{00} & \mathbf{h}_{01} & \dots \\ 0 & 0 & \mathbf{h}_{01}^\dagger & \mathbf{h}_{00} & \dots \\ \vdots & \vdots & \vdots & \vdots & \ddots \end{pmatrix} \quad \mathbf{H_1} = \begin{pmatrix} \mathbf{h}_1 & 0 & 0 & 0 & \dots \\ 0 & \mathbf{h}_1 & 0 & 0 & \dots \\ 0 & 0 & \mathbf{h}_1 & 0 & \dots \\ 0 & 0 & 0 & \mathbf{h}_1 & \dots \\ \vdots & \vdots & \vdots & \vdots & \ddots \end{pmatrix} . \tag{2.25}$$

Depending on the boundary condition $\mathbf{H}_0$ varies. In the (a) case $\mathbf{H}_0$ is a $3W \times 3W$ matrix with a $\mathbf{h}_{01}^\dagger$ in the top right corner and a $\mathbf{h}_{01}$ in the bottom left corner. In the (b) case we have the same but with zeros in those corners. In the (c) case there are two extra rows and columns in $\mathbf{H}_0$. We can think of it as a $W + 1$ (b) case where the last row and last column is eliminated. For a visual representation of the (c) case presented on figure 2.6, see figure 2.8 where the non-zero hoppings are shown with black squares. Also for the same case the full $\hat{\mathbf{H}}$ Hamiltonian of length $L = 3$ (where L is the number of unit cells in the x direction) can be seen on figure 2.9.

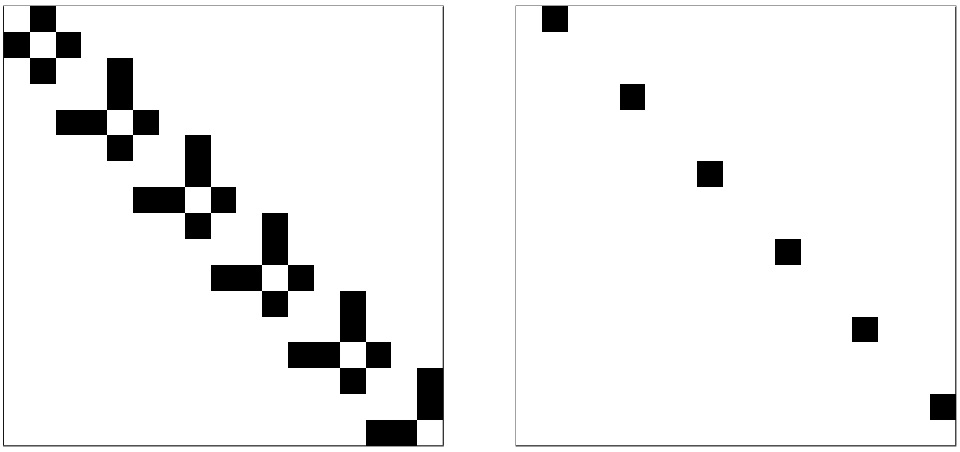

(a) $\mathbf{H}_0$ (b) $\mathbf{H}_1$

Figure 2.8: The matrices used to construct the strip. The black squares represent -1 and the white region represents 0.

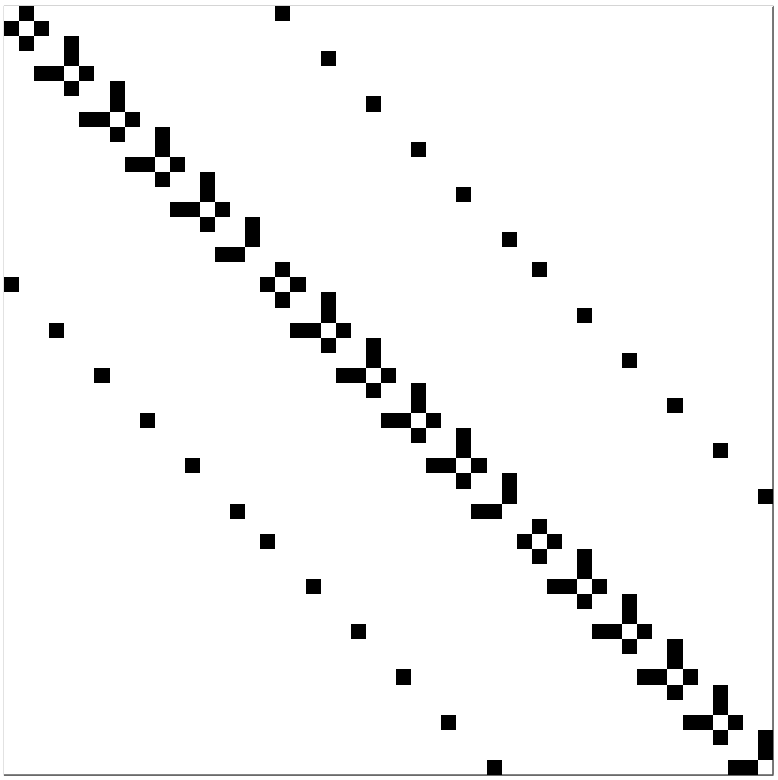

Figure 2.9: The Hamiltonian $\hat{\mathbf{H}}$ for $L = 3$ $W = 5$. The black squares represent -1 and the white region represents 0.

2.3.1 Dispersion relation

First we want to solve the eigenvalue problem of the $\hat{\mathbf{H}}$ Hamiltonian. The eigenvector $\mathbf{\Psi}$ can be divided in sections, and be described as a two-dimensional array Ψ_p^n. Here $n \in \mathbf{Z}$ denotes the n-th $\mathbf{H}_0$ block (unit cell) and $p \in \{1, 2, .., M\}$ goes over the degrees of freedom inside one site. The degrees of freedom M are either $3W$ or $3W + 2$ depending on the boundary condition. Respectively the $\hat{\mathbf{H}}$ Hamiltonian can be thought of as a four-dimensional array H_{pq}^{nm} where:

$$H_{pq}^{nm} = \delta_{nm} H_{pq}^{(0)} + \delta_{n+1,m} H_{pq}^{(1)} + \delta_{n,m+1} H_{pq}^{(1)\dagger} \ . \tag{2.26}$$

Applying this to a two-dimensional array we get the following:

$$\sum_{m,q} H_{pq}^{nm} \Psi_q^m = \sum_q (H_{pq}^{(0)} \Psi_q^n + H_{pq}^{(1)} \Psi_q^{n-1} + H_{pq}^{(1)\dagger} \Psi_q^{n+1}). \tag{2.27}$$

The following ansatz will be used:

$$\Psi_p^n(k) = \mathrm{e}^{ikn} \Phi_p \ . \tag{2.28}$$

Substituting this in (2.27) we get:

$$\sum_{m,q} H_{pq}^{nm} \Psi_q^m = \mathrm{e}^{ikn} \sum_q (H_{pq}^{(0)} \Phi_q + \mathrm{e}^{ik} H_{pq}^{(1)} \Phi_q + \mathrm{e}^{-ik} H_{pq}^{(1)\dagger} \Phi_q) \tag{2.29}$$

With a more transparent notation where $|\Phi\rangle \equiv (\Phi_1, \Phi_2, ..., \Phi_M)$:

$$(\hat{\mathbf{H}}\mathbf{\Psi})^n = \mathrm{e}^{ikn} (\mathbf{H}_0 |\Phi\rangle + \mathrm{e}^{ik} \mathbf{H}_1 |\Phi\rangle + \mathrm{e}^{-ik} \mathbf{H}_1^\dagger |\Phi\rangle) \tag{2.30}$$

The $\mathbf{H}\mathbf{\Psi} = E\mathbf{\Psi}$ eigenvalue problem this way translates to:

$$\mathbf{H}_0 |\Phi\rangle + \mathrm{e}^{ik} \mathbf{H}_1 |\Phi\rangle + \mathrm{e}^{-ik} \mathbf{H}_1^\dagger |\Phi\rangle = E |\Phi\rangle \ . \tag{2.31}$$

Now this is an eigenvalue problem of an $M \times M$ matrix, which can be solved numerically. This will give M eigenvalues and eigenvectors for every k wave-vector $E_p(k), p \in \{1, 2, ..., M\}$.

The dispersion relation in the case of periodic boundary condition is the same as in the infinite Lieb-lattice (2.10) where $k_x \equiv k$ and $k_y \in \{0, 2\pi/W, 2\pi/W \cdot 2,$ $..., 2\pi/W \cdot (W - 1)\}$. for every k there are W bands above 0, W bands below 0

and W flat bands. The other two boundary conditions can't be solved this way. We can see numerical solutions for the cases presented in figure 2.6 (b) and (c) on figure 2.10, also for a larger system on figure 2.11.

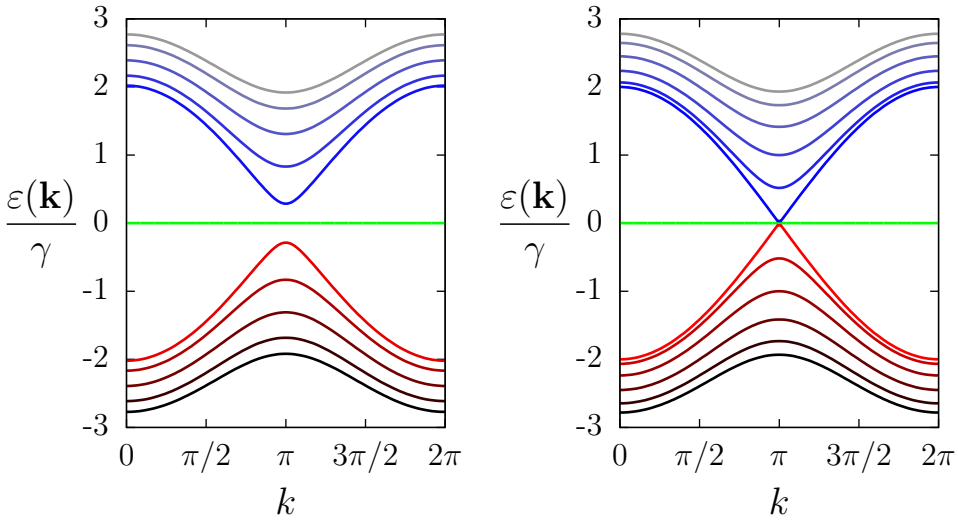

(a) *hanging* boundary (b) *closed* boundary

Figure 2.10: Dispersion relation of a Lieb lattice strip of width $W = 5$ with two different boundary condition. There are 5 degenerated flat bands in each case.

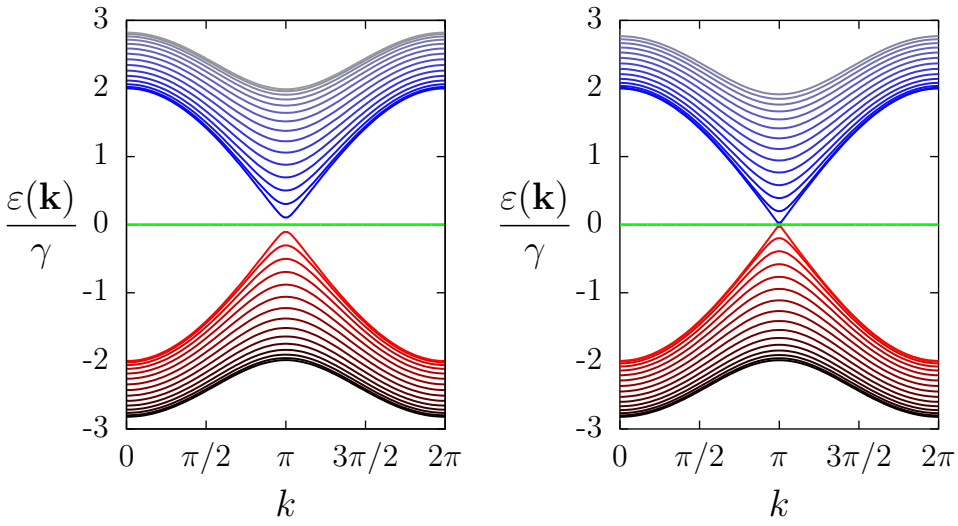

(a) *hanging* boundary (b) *closed* boundary

Figure 2.11: Dispersion relation of a Lieb lattice strip of width $W = 15$ with two different boundary condition. There are 15 degenerated flat bands in each case.

As we can see the two boundary conditions make a very important difference in the dispersion relation. The *hanging* boundary condition has a gap at $k = \pi$ while the *closed* boundary condition is always gapless. In the case of periodic boundary condition we can have both characteristics depending on the parity of W. If W is even, k_y can equal π thus the Dirac points is included so the dispersion relation is gapless. If W is odd, k_y can't equal π so there will be a gap. The nearest point to the Dirac point is $k_y = \pi \pm \pi/W$, thus the gap is approximately π/W. Similarly in the *hanging* boundary condition we see that the gap decreases as the width of the strip increases.

2.3.2 Number of open channels

It is useful to define the number of open channels $\mathcal{N}$ for later uses. At a given energy the number of open channels is the number of possible propagating states ($k \in \mathbb{R}$) with positive group velocity at the given energy. We can simply count these by drawing an $E = const.$ line on the dispersion relation and counting the intersections and taking the half of it. We can see a simple example for this on figure 2.12.

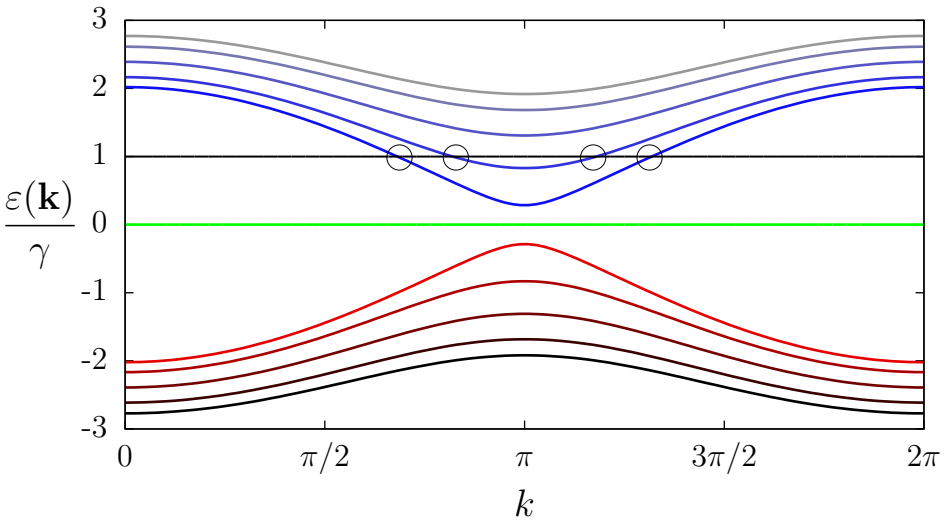

Figure 2.12: The dispersion relation seen on figure 2.10 with showing the propagating modes at $E = 1$ energy. The number of open channels at this energy is $\mathcal{N} = 2$.

On figure 2.13 we can see the number of open channels for the two boundary conditions for different W values. We can see the difference near zero energy caused by the gap. It is also visible that the gap becomes smaller for wider

strips. The maximum of the number of open channels is at $E = 2\gamma$ energy. This is the energy where the 2.10 dispersion relation has a saddle point.

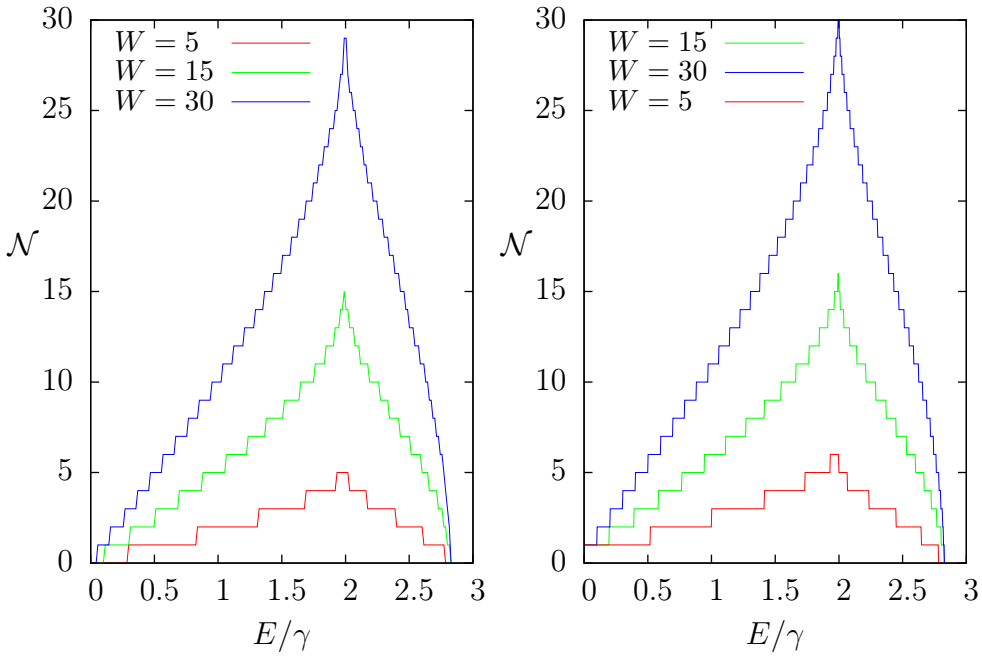

(a) *hanging* boundary (b) *closed* boundary

Figure 2.13: The number of open channels for different boundary conditions and different widths W. Only the positive energies are shown, for the negative energies the spectrum is symmetric.

2.3.3 Hamiltonian of disordered Lieb lattice ribbon

We will see in section 5.1 that in the actual calculation we will be using an infinite strip of pure Lieb lattice, where in a finite L length region we introduce disordered. In our calculations we use the Anderson model for the disorder [9]. The disorder affects only the on-site potentials. The on-site potential of every disordered site is a random number selected from a uniform distribution $\varepsilon_s \in [-\varepsilon_d, \varepsilon_d]$.

3 Landauer-Büttiker formalism

In this chapter the basics of the Landauer-Büttiker formalism will be discussed. This formalism can be used to calculate electric transport in quantum mechanical systems. By calculating the Green's function of the system it is possible to obtain it's conductance. In this thesis only a two terminal system on lattice will be discussed at $T = 0\,\mathrm{K}$ temperature, but the general formalism can be extended to multiterminal systems with finite temperature too. For further readings about the whole formalism and applications see: [10], [4], [5]

3.1 Landauer formula

First let's take a ballistic conductor of length L and width W. The conductor is connected to two reflectionless contacts having chemical potential μ_1 and μ_2. In this case the current through the conductor can be calculated as (for derivation see [10]):

$$I_c = \frac{2e^2}{h} \cdot \mathcal{N} \cdot \frac{\mu_2 - \mu_1}{e} \ , \tag{3.1}$$

where $\mathcal{N}$ is the number of open channels in the conductor. The difference in chemical potential is achieved through a voltage difference $eV = \mu_2 - \mu_1$. So the contact conductance or contact resistance can be calculated as:

$$G_c = \frac{2e^2}{h}\mathcal{N} \qquad\qquad R_c = \frac{h}{2e^2\mathcal{N}} = \frac{12.9}{\mathcal{N}}\mathrm{k}\Omega \ . \tag{3.2}$$

Of course this is only the case if there is no scattering in the conductor. If there is scattering we can think of it the following way. The system consist of two contacts a scattering region and two leads (wires) connecting the contacts to the scattering region. The leads are assumed to be ballistic, and the contacts are assumed to be reflectionless. This is the so called two terminal setup (see figure 3.1).

Figure 3.1: Schematic figure of a two terminal setup. μ_1 and μ_2 are the chemical potentials in the contacts. L and R are the left and right leads.

In a two terminal setup every open channel of the first lead has transmission probabilities to scatter in the open channels of the second lead. By knowing this transmission probabilities the Landauer formula can be expressed as:

$$G = \frac{2e^2}{h} \sum_{p}^{\mathcal{N}_1} \sum_{q}^{\mathcal{N}_2} T_{qp} =: G_o \bar{T}_{21} \tag{3.3}$$

where T_{qp} is transmission probability from the p-th open channel in the first lead to the q-t open channel in the second lead (actually the transmission probabilities normalized with the fraction of group velocities $|v_q|/|v_p|$ as explained in detail in [10]). $G_o = 2e^2/h$ is the conductance quantum and $\bar{T}_{21}$ is the transmission function from the first to the second terminal. The transmission function is an energy dependent quantity. For the 0 K temperature transport it can be shown that the transmission function on the Fermi energy can be used.

The transmission function can be calculated from the scattering matrix ($\mathbf{S}$). The scattering matrix gives the relation of the incoming channels to the outgoing channels (see figure 3.2 for a visual representation):

$$\mathbf{o} = \mathbf{S} \cdot \mathbf{i} \ . \tag{3.4}$$

In a two terminal system the S-matrix can be partitioned in the following way. First we divide the $\mathbf{i}$ and $\mathbf{o}$ vectors in two sections:

$$\mathbf{i} = \begin{pmatrix} \mathbf{i}_L \\ \mathbf{i}_R \end{pmatrix} \qquad \mathbf{o} = \begin{pmatrix} \mathbf{o}_L \\ \mathbf{o}_R \end{pmatrix} \ , \tag{3.5}$$

where $\mathbf{i}_{L/R}$ are the incoming channels and $\mathbf{o}_{L/R}$ are the outgoing channels on the

Figure 3.2: Visual representation of the S-matrix. i_p-s are the incoming channels, and o_p-s are the outgoing channels.

left/right terminals. With this the S-matrix is partitioned as:

$$\mathbf{S} =: \begin{pmatrix} \mathbf{r} & \mathbf{t}' \\ \mathbf{t} & \mathbf{r}' \end{pmatrix} \ . \tag{3.6}$$

Here $\mathbf{r}$ contains the reflexion amplitudes and $\mathbf{t}$ contains the transmission amplitudes. From the viewpoint of electric transport we are interested in the scattering from $\mathbf{i}_L$ to $\mathbf{o}_R$. This is described by $\mathbf{t}$ as:

$$\mathbf{o}_R = \mathbf{t} \cdot \mathbf{i}_L \ . \tag{3.7}$$

The transmission probabilities are the absolute square of the transmission amplitudes. With this the transmission function can be calculated as:

$$\bar{T}_{21} = \sum_{p}^{\mathcal{N}_1} \sum_{q}^{\mathcal{N}_2} T_{qp} = \sum_{p}^{\mathcal{N}_1} \sum_{q}^{\mathcal{N}_2} |t_{qp}|^2 = \mathrm{Tr}\big(\mathbf{t}\mathbf{t}^\dagger\big) \ . \tag{3.8}$$

This means that the conductance can be calculated if the S-matrix is known for a given system. In the followings a formalism will be shown to determine the S-matrix for a tight binding system.

3.2 Eigenvalue problem of generalised leads

We will start with the eigenvalue problem of an infinite generalised lead. A generalised lead can be thought of as a linear chain, where every node has multiple degrees of freedom. This is the same description we used in section 2.3 for the infinite strip of Lieb lattice, but now for an arbitrary lattice. The Hamiltonian of a generalised lead looks like (2.22):

$$\hat{\mathbf{H}} = \begin{pmatrix} \mathbf{H}_0 & \mathbf{H}_1 & 0 & 0 & \dots \\ \mathbf{H}_1^\dagger & \mathbf{H}_0 & \mathbf{H}_1 & 0 & \dots \\ 0 & \mathbf{H}_1^\dagger & \mathbf{H}_0 & \mathbf{H}_1 & \dots \\ 0 & 0 & \mathbf{H}_1^\dagger & \mathbf{H}_0 & \dots \\ \vdots & \vdots & \vdots & \vdots & \ddots \end{pmatrix} , \tag{3.9}$$

where now $\mathbf{H}_0$ is an arbitrary $M \times M$ Hermitian matrix and $\mathbf{H}_1$ is an arbitrary $M \times M$ matrix, where M is the degrees of freedom in one node. Of course in our calculations $\mathbf{H}_0$ and $\mathbf{H}_1$ will be the previously defined ones (2.25). If we want to solve the eigenvalue problem of the $\hat{\mathbf{H}}$ Hamiltonian we could use the method showed in the previous chapter at section (2.22) and use

$$\left(\mathbf{H}_0 + \mathrm{e}^{ik}\mathbf{H}_1 + \mathrm{e}^{-ik}\mathbf{H}_1^\dagger\right)|\Phi\rangle = E\,|\Phi\rangle \tag{3.10}$$

to calculate the eigenvalues. This will give M eigenvalues and eigenvectors for every k wavevector. In this case the energies are parametrized by k. In the case of Green functions we want to do the opposite and use the energy as a parameter, so we want to know the eigenvectors at a given energy, and not at a given wavenumber. To do this we can use the following trick. Lets introduce a new $|\Theta\rangle$ vector the following way:

$$|\Theta\rangle := \mathrm{e}^{-ik}\,|\Phi\rangle \tag{3.11}$$

Now equations (3.10) and (3.11) can be united to form a generalised eigenvalue problem:

$$\begin{pmatrix} E\cdot\mathbf{I} - \mathbf{H}_0 & -\mathbf{H}_1 \\ \mathbf{I} & \mathbf{0} \end{pmatrix} \begin{pmatrix} |\Phi\rangle \\ |\Theta\rangle \end{pmatrix} = \mathrm{e}^{ik} \begin{pmatrix} \mathbf{H}_1 & \mathbf{0} \\ \mathbf{0} & \mathbf{I} \end{pmatrix} \begin{pmatrix} |\Phi\rangle \\ |\Theta\rangle \end{pmatrix} . \tag{3.12}$$

The solution of this problem is easy if $\mathbf{H}_1$ is invertible. Since we can multiply the first rows with the inverse and get a normal eigenvalue problem. But unfortu-

nately this is not the case for our $\mathbf{H}_1$ in (2.25). We will get back to this problem in section 3.2.1. For now let's assume that we have solved the eigenvalue problem. Since now we have a $2M \times 2M$ matrix we will have $2M$ eigenvalues. So for a given E energy we have $2M$ eigenstates characterised by $2M$ wavenumbers. It is useful to introduce the group velocity of a state calculated as:

$$\begin{aligned} v(k) &:= \partial_k E(k) = \partial_k \left\langle \Phi \right| \mathbf{H}_0 + \mathrm{e}^{ik}\mathbf{H}_1 + \mathrm{e}^{-ik}\mathbf{H}_1^\dagger \left| \Phi \right\rangle \\ &= i \left\langle \Phi \right| \mathrm{e}^{ik}\mathbf{H}_1 - \mathrm{e}^{-ik}\mathbf{H}^\dagger \left| \Phi \right\rangle \ , \end{aligned} \tag{3.13}$$

the last equality is true because $\partial_k \langle \Phi | \Phi \rangle = 0$. We will group our states using the following properties. We will have propagating modes if $\mathrm{Im}(k) = 0$ or evanescent modes if $\mathrm{Im}(k) \neq 0$. Depending on the sign of the group velocity of the propagating modes we will have $|+\rangle$ and $|-\rangle$ states. In the case of evanescent modes the sign of $\mathrm{Im}(k)$ will be the characterizing property. With this we will have $|\sigma_p\rangle$ ($\sigma \in \{+,-\}$ and $p \in \{1,2,...,M\}$) states, with wavenumbers k_p^σ.

The eigenstates $|\sigma_p\rangle$ are not necessarily orthogonal to each other since they come from the (3.12) generalised eigenvalue problem. It is useful to define the dual states ($\langle\tilde{\sigma}_p|$) using the following relation:

$$\langle \tilde{\sigma}_p | \sigma_q \rangle = \delta_{pq} \ . \tag{3.14}$$

This can be calculated numerically as a matrix inverse.

3.2.1 Eigenvalue problem with singular $\mathbf{H}_1$

We saw that solving the generalised eigenvalue problem (3.12) is not straightforward if the $\mathbf{H}_1$ matrix is singular. To overcome this problem we can use the so called singular value decomposition (SVD). Here a brief introduction will be shown for the method without any proofs. For a more detailed explanation see [11]. Our singular matrix can be expressed as:

$$\mathbf{H}_1 = \mathbf{U}\mathbf{\Sigma}\mathbf{V}^\dagger \ , \tag{3.15}$$

where $\mathbf{U}$ and $\mathbf{V}$ are unitary matrices and $\mathbf{\Sigma}$ is a diagonal matrix. $\mathbf{\Sigma}$ contains the singular values of $\mathbf{H}_1$ (the square roots of the eigenvalues of $\mathbf{H}_1\mathbf{H}_1^\dagger$). The singularity of $\mathbf{H}_1$ is caused by the zero elements in the diagonal of $\mathbf{\Sigma}$. We can

define the following matrices using $\mathbf{U}$ and $\mathbf{V}$:

$$\hat{\mathbf{U}} = \begin{pmatrix} \mathbf{U} & \mathbf{0} & \mathbf{0} & \mathbf{0} & \dots \\ \mathbf{0} & \mathbf{U} & \mathbf{0} & \mathbf{0} & \dots \\ \mathbf{0} & \mathbf{0} & \mathbf{U} & \mathbf{0} & \dots \\ \mathbf{0} & \mathbf{0} & \mathbf{0} & \mathbf{U} & \dots \\ \vdots & \vdots & \vdots & \vdots & \ddots \end{pmatrix}, \qquad \hat{\mathbf{V}} = \begin{pmatrix} \mathbf{V} & \mathbf{0} & \mathbf{0} & \mathbf{0} & \dots \\ \mathbf{0} & \mathbf{V} & \mathbf{0} & \mathbf{0} & \dots \\ \mathbf{0} & \mathbf{0} & \mathbf{V} & \mathbf{0} & \dots \\ \mathbf{0} & \mathbf{0} & \mathbf{0} & \mathbf{V} & \dots \\ \vdots & \vdots & \vdots & \vdots & \ddots \end{pmatrix}, \tag{3.16}$$

Since $\hat{\mathbf{U}}$ is a unitary matrix we can use it as a unitary transformation on $\hat{\mathbf{H}}$ without affecting the eigenvalues:

$$\hat{\mathbf{H}} \to \hat{\mathbf{U}}^\dagger \hat{\mathbf{H}} \hat{\mathbf{U}} \tag{3.17}$$

$$\mathbf{H}_0 \to \mathbf{U}^\dagger \mathbf{H}_0 \mathbf{U} \tag{3.18}$$

$$\mathbf{H}_1 \to \mathbf{U}^\dagger \mathbf{H}_1 \mathbf{U} = \mathbf{\Sigma} \mathbf{V}^\dagger \mathbf{U} \ . \tag{3.19}$$

By rearranging the indices we can get the following partitioning for $\mathbf{\Sigma}$:

$$\mathbf{\Sigma} =: \begin{pmatrix} \mathbf{\Sigma}^n & \mathbf{0} \\ \mathbf{0} & \mathbf{0} \end{pmatrix}, \tag{3.20}$$

where $\mathbf{\Sigma}^n$ contains only nonzero element in the diagonal. With this the partitioning of $\mathbf{H}_0$ and $\mathbf{H}_1$ will be the following:

$$\mathbf{H}_0 =: \begin{pmatrix} \mathbf{H}_0^n & \mathbf{A} \\ \mathbf{A}^\dagger & \mathbf{H}_0^d \end{pmatrix} \qquad \mathbf{H}_1 =: \begin{pmatrix} \mathbf{H}_1^n & \mathbf{B} \\ \mathbf{0} & \mathbf{0} \end{pmatrix} \ . \tag{3.21}$$

Now the sites described by $\mathbf{H}_0^d$ can be eliminated using the so called decimation. You can read about the process in detail in appendix B. After the decimation we will have an effective reduced Hamiltonian that is energy dependent, but the eigenvalues of the original $\hat{\mathbf{H}}$ Hamiltonian are unaffected. The new Hamiltonian will have the same linear chain structure and the new energy dependent $\tilde{\mathbf{H}}_0$ and $\tilde{\mathbf{H}}_1$ Hamiltonians will be:

$$\begin{aligned} \tilde{\mathbf{H}}_0 &= \mathbf{H}_0^n + \mathbf{A}(E \cdot \mathbf{I} - \mathbf{H}_0^d)^{-1} \mathbf{A}^\dagger + \mathbf{B}(E \cdot \mathbf{I} - \mathbf{H}_0^d)^{-1} \mathbf{B}^\dagger \\ \tilde{\mathbf{H}}_1 &= \mathbf{H}_1^n + \mathbf{B}(E \cdot \mathbf{I} - \mathbf{H}_0^d)^{-1} \mathbf{A}^\dagger \ . \end{aligned} \tag{3.22}$$

With this new decimated Hamiltonian the (3.12) generalised eigenvalue problem can be solved since it can be shown that the new $\tilde{\mathbf{H}}_1$ Hamiltonian is not singular.

We can see the whole process of SVD and decimation schematically on figure 3.3.

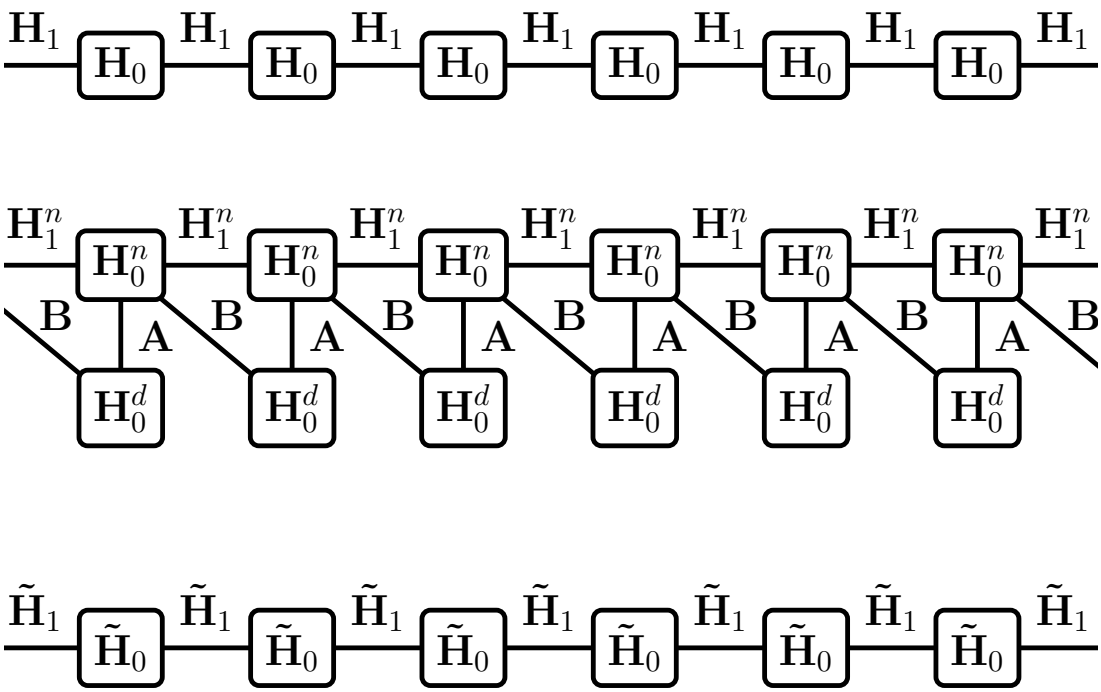

Figure 3.3: Schematic representation of the SVD and decimation. We start with the top linear chain. After the SVD we get the structure shown in the middle chain. After decimating the $\mathbf{H}_0^d$ sites we end up with a linear structure shown at the bottom. While the original $\mathbf{H}_1$ matrix was singular, in the new chain the $\tilde{\mathbf{H}}_1$ is invertible.

It is important to note here, that this works for an infinite lead. But for our purposes only a semi infinite lead will be used. In that case this method should be slightly modified. In the bulk of the lead the previous statements are correct, but for the edge of the lead the $\tilde{\mathbf{H}}_0$ is not the same as in 3.22. But instead it will be:

$$\tilde{\mathbf{H}}_0' = \mathbf{H}_0^n + \mathbf{A}(E \cdot \mathbf{I} - \mathbf{H}_0^d)^{-1}\mathbf{A}^\dagger \ . \tag{3.23}$$

This means that the actual system will be like the one we can see on figure 3.4

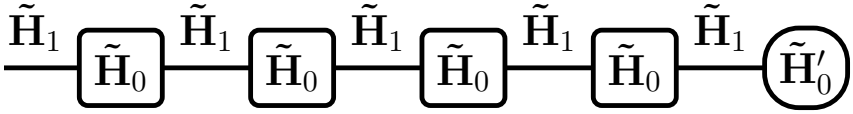

Figure 3.4: Structure of the decimated semi-infinite lead.

In the actual numerics we will use the bulk part as leads and we will put the last node ($\tilde{\mathbf{H}}_0'$) in the scattering region.

3.3 Green's function of generalised leads

Let's assume that we already have on hand $|\sigma_p\rangle$, $\langle\tilde{\sigma}_p|$ and k_p^σ. The Green's function ($G(E)$) is defined through the following equation:

$$(E\cdot\hat{\mathbf{I}}-\hat{\mathbf{H}})\hat{\mathbf{G}}=\hat{\mathbf{I}}\ , \tag{3.24}$$

and with index notation:

$$\sum_{\ell,r}(E\cdot\delta_{pr}^{n\ell}-H_{pr}^{n\ell})G_{rq}^{\ell m}=\delta_{pq}^{nm}\ . \tag{3.25}$$

If we substitute the (2.26) Hamiltonian in this equation we get the following:

$$(E\cdot\mathbf{I}-\mathbf{H}_0)\mathbf{G}^{nm}-\mathbf{H}_1\mathbf{G}^{n+1,m}-\mathbf{H}_1^\dagger\mathbf{G}^{n-1,m}=\mathbf{I}^{nm}\ . \tag{3.26}$$

It can be shown that the following Green's function satisfies this equation:

$$\mathbf{G}^{nm}=\begin{cases}\sum_{p=1}^{M}\mathrm{e}^{ik_p^-(n-m)}\left|-_p\right\rangle\left\langle\tilde{-}_p\right|\mathbf{V}^{-1} & \text{for}\quad n\le m\\ \sum_{p=1}^{M}\mathrm{e}^{ik_p^+(n-m)}\left|+_p\right\rangle\left\langle\tilde{+}_p\right|\mathbf{V}^{-1} & \text{for}\quad n\ge m\end{cases}\ , \tag{3.27}$$

where the $\mathbf{V}$ matrix can be calculated as:

$$\mathbf{V}=\sum_{p=1}^{M}\mathbf{H}_1^\dagger\left[\mathrm{e}^{-ik_p^+}\left|+_p\right\rangle\left\langle\tilde{+}_p\right|-\mathrm{e}^{-ik_p^-}\left|-_p\right\rangle\left\langle\tilde{-}_p\right|\right]\ . \tag{3.28}$$

In the case of two terminal transport calculations we need the Green's function of a semi-infinite lead. We can have two different type of leads depending of which sites we eliminate. In the case where the sites $n\ge n_0$ are missing we will call the Green's function $\mathbf{G}_L^{nm}$, and in the case where $n\le n_0$ $\mathbf{G}_R^{nm}$. We can address this problems as a boundary condition problem, where:

$$\mathbf{G}_{L/R}^{n_0,m}=0\quad\text{for}\quad m\lessgtr n_0\ . \tag{3.29}$$

This can be achieved using the following Green's functions:

$$\mathbf{G}_L^{nm} = \mathbf{G}^{nm} - \sum_{p,q=1}^{M} |-_q\rangle \, \mathrm{e}^{ik_q^-(n-n_0)} \, \langle \tilde{-}_q|+_p\rangle \, \mathrm{e}^{ik_p^+(n_0-m)} \, \langle \tilde{+}| \, \mathbf{V}^{-1}$$

$$\mathbf{G}_R^{nm} = \mathbf{G}^{nm} - \sum_{p,q=1}^{M} |+_q\rangle \, \mathrm{e}^{ik_q^+(n-n_0)} \, \langle \tilde{+}_q|-_p\rangle \, \mathrm{e}^{ik_p^-(n_0-m)} \, \langle \tilde{-}| \, \mathbf{V}^{-1} \ . \tag{3.30}$$

In the practical calculations we will be only interested in the Green's function on the edge of the leads. This means that the following two matrices are important:

$$\mathbf{G}_L^{n_0-1,n_0-1} = \left[\mathbf{I} - \sum_{p,q=1}^{M} |-_q\rangle \, \mathrm{e}^{-ik_q^-} \, \langle \tilde{-}_q|+_p\rangle \, \mathrm{e}^{ik_p^+} \, \langle \tilde{+}_p| \right] \mathbf{V}^{-1}$$

$$\mathbf{G}_R^{n_0+1,n_0+1} = \left[\mathbf{I} - \sum_{p,q=1}^{M} |+_q\rangle \, \mathrm{e}^{ik_q^+} \, \langle \tilde{+}_q|-_p\rangle \, \mathrm{e}^{-ik_p^-} \, \langle \tilde{-}_p| \right] \mathbf{V}^{-1} \ . \tag{3.31}$$

3.4 Dyson equation

With the previously explained formalism we can calculate numerically the Green's function of the leads that connect to the scattering region. Now we want to calculate the Green's function of the whole system. For this we can use the Dyson equation. Let's build up our system like the followings. The $\boldsymbol{\mathcal{H}}_0$ Hamiltonian describes the two leads and the scattering region, but without any connection between the three. This means that it can be chosen to be block diagonal:

$$\boldsymbol{\mathcal{H}}_0 = \begin{pmatrix} \hat{\mathbf{H}}_L & \mathbf{0} & \mathbf{0} \\ \mathbf{0} & \hat{\mathbf{H}}_R & \mathbf{0} \\ \mathbf{0} & \mathbf{0} & \hat{\mathbf{H}}_S \end{pmatrix} \ , \tag{3.32}$$

where $\hat{\mathbf{H}}_L$ and $\hat{\mathbf{H}}_R$ are the Hamiltonians of the leads on the left and right side and $\hat{\mathbf{H}}_S$ is the Hamiltonian of the scattering region. The connection between the leads and the scattering region is described by $\boldsymbol{\mathcal{H}}_1$:

$$\boldsymbol{\mathcal{H}}_1 = \begin{pmatrix} \mathbf{0} & \mathbf{0} & \hat{\mathbf{\Gamma}}_L \\ \mathbf{0} & \mathbf{0} & \hat{\mathbf{\Gamma}}_R \\ \hat{\mathbf{\Gamma}}_L^\dagger & \hat{\mathbf{\Gamma}}_R^\dagger & \mathbf{0} \end{pmatrix} \ , \tag{3.33}$$

where $\hat{\mathbf{\Gamma}}_L$ and $\hat{\mathbf{\Gamma}}_R$ describes the hoppings from the left/right lead to the scattering

region. The equation defining the Green's function is the following:

$$(E \cdot \boldsymbol{\mathcal{I}} - \boldsymbol{\mathcal{H}}_0 - \boldsymbol{\mathcal{H}}_1)\boldsymbol{\mathcal{G}} = \boldsymbol{\mathcal{I}} \tag{3.34}$$

We can also define the Green's function of the $\boldsymbol{\mathcal{H}}_0$ system as:

$$(E \cdot \boldsymbol{\mathcal{I}} - \boldsymbol{\mathcal{H}}_0)\boldsymbol{\mathcal{G}}_0 = \boldsymbol{\mathcal{I}} \ . \tag{3.35}$$

Since $\boldsymbol{\mathcal{H}}_0$ is block diagonal the corresponding Green's function will also be block diagonal:

$$\boldsymbol{\mathcal{G}}_0 = \begin{pmatrix} \hat{\mathbf{G}}_L & \mathbf{0} & \mathbf{0} \\ \mathbf{0} & \hat{\mathbf{G}}_R & \mathbf{0} \\ \mathbf{0} & \mathbf{0} & \hat{\mathbf{G}}_S \end{pmatrix} \ , \tag{3.36}$$

where $\hat{\mathbf{G}}_L$ and $\hat{\mathbf{G}}_R$ are the previously derived Green's functions for the left and right leads (3.30). And $\hat{\mathbf{G}}_S$ can be calculated using:

$$\hat{\mathbf{G}}_S = (E \cdot \mathbf{I} - \hat{\mathbf{H}}_S)^{-1} \ . \tag{3.37}$$

With this the (3.34) equation becomes:

$$(\boldsymbol{\mathcal{I}} - \boldsymbol{\mathcal{G}}_0\boldsymbol{\mathcal{H}}_1)\boldsymbol{\mathcal{G}} = \boldsymbol{\mathcal{G}}_0 \ . \tag{3.38}$$

With a matrix inversion we get the Dyson equation as:

$$\boldsymbol{\mathcal{G}} = (\boldsymbol{\mathcal{G}}_0^{-1} - \boldsymbol{\mathcal{H}}_1)^{-1} \tag{3.39}$$

The problem with this equation now is that we have to compute the inverse of an infinite matrix. We will see in the next section that for the transport calculations we will not need the whole $\boldsymbol{\mathcal{G}}$ Green's function, but only the elements on the edge of the scattering region. We will show that it is enough to compute the inverse of a finite matrix to compute these elements, and thus the calculation can be done numerically.

First we have to look at the structure of the $\boldsymbol{\mathcal{G}}_0$ and $\boldsymbol{\mathcal{H}}_1$ matrices. We rearrange the sites in a way that in the bottom right corner we have the scattering region and the edge of the leads. With this the two matrices will look like the following:

$$\boldsymbol{\mathcal{G}}_0 = \left(\begin{array}{cc|cc|c} \hat{\mathbf{g}}^B_{0L} & \mathbf{0} & \hat{\mathbf{g}}^{BE}_{0L} & \mathbf{0} & \mathbf{0} \\ \mathbf{0} & \hat{\mathbf{g}}^B_{0R} & \mathbf{0} & \hat{\mathbf{g}}^{BE}_{0R} & \mathbf{0} \\ \hline \hat{\mathbf{g}}^{BE\dagger}_{0L} & \mathbf{0} & \hat{\mathbf{g}}^E_{0L} & \mathbf{0} & \mathbf{0} \\ \mathbf{0} & \hat{\mathbf{g}}^{BE\dagger}_{0R} & \mathbf{0} & \hat{\mathbf{g}}^E_{0R} & \mathbf{0} \\ \mathbf{0} & \mathbf{0} & \mathbf{0} & \mathbf{0} & \hat{\mathbf{G}}_S \end{array}\right) =: \begin{pmatrix} \hat{\mathbf{g}}^B_0 & \hat{\mathbf{g}}^{BE}_0 \\ \hat{\mathbf{g}}^{BE\dagger}_0 & \hat{\mathbf{g}}_0 \end{pmatrix} , \tag{3.40}$$

$$\boldsymbol{\mathcal{H}}_1 = \left(\begin{array}{cc|ccc} \mathbf{0} & \mathbf{0} & \mathbf{0} & \mathbf{0} & \mathbf{0} \\ \mathbf{0} & \mathbf{0} & \mathbf{0} & \mathbf{0} & \mathbf{0} \\ \hline \mathbf{0} & \mathbf{0} & \mathbf{0} & \mathbf{0} & \boldsymbol{\gamma}_L \\ \mathbf{0} & \mathbf{0} & \mathbf{0} & \mathbf{0} & \boldsymbol{\gamma}_R \\ \mathbf{0} & \mathbf{0} & \boldsymbol{\gamma}^\dagger_L & \boldsymbol{\gamma}^\dagger_R & \mathbf{0} \end{array}\right) =: \begin{pmatrix} \mathbf{0} & \mathbf{0} \\ \mathbf{0} & \hat{\mathbf{h}}_1 \end{pmatrix} , \tag{3.41}$$

where we introduced $\hat{\mathbf{g}}^B_{0L/R}$ which is the Green's function inside the leads, $\hat{\mathbf{g}}^E_{0L/R}$ which is the surface Green's function of the leads (this is what we derived in (3.31)) and $\hat{\mathbf{g}}^{BE}_{0L/R}$ is the connection between the previous two. The $\boldsymbol{\gamma}_{L/R}$ matrices are the hoppings between the edge of the leads and the scattering region. We can partition the $\boldsymbol{\mathcal{G}}$ matrix similarly as:

$$\boldsymbol{\mathcal{G}} =: \begin{pmatrix} \hat{\mathbf{g}}^B & \hat{\mathbf{g}}^{BE} \\ \hat{\mathbf{g}}^{BE\dagger} & \hat{\mathbf{g}} \end{pmatrix} . \tag{3.42}$$

For the transport calculation the part that we are interested in is $\hat{\mathbf{g}}$. If we put these partitionings in the (3.38) equation we get the following equation for $\hat{\mathbf{g}}$:

$$(\hat{\mathbf{I}} - \hat{\mathbf{g}}_0\hat{\mathbf{h}}_1)\hat{\mathbf{g}} = \hat{\mathbf{g}}_0 . \tag{3.43}$$

This means that the we have an equation of the same structure as in the (3.39) Dyson equation but now the finite $\hat{\mathbf{g}}_0$ and $\hat{\mathbf{h}}_1$ can be used:

$$\hat{\mathbf{g}} = (\hat{\mathbf{g}}_0^{-1} - \hat{\mathbf{h}}_1)^{-1} . \tag{3.44}$$

3.5 Fischer-Lee relations

The previous sections explained how the $\mathbf{g}$ Green's function can be calculated. Now we will give a formula for calculating the S-matrix if the $\mathbf{g}$ Green's function

is known. First let's partition $\mathbf{g}$ the same way we can partition $\mathbf{g}_0$ in (3.40) as:

$$\mathbf{g} =: \begin{pmatrix} \mathbf{g}^E & \mathbf{g}^{ES} \\ \mathbf{g}^{ES\dagger} & \mathbf{g}^S \end{pmatrix} \qquad \mathbf{g}^E =: \begin{pmatrix} \mathbf{g}^E_{LL} & \mathbf{g}^E_{LR} \\ \mathbf{g}^E_{RL} & \mathbf{g}^E_{RR} \end{pmatrix} , \tag{3.45}$$

Where $\mathbf{g}^E$ is the surface Green's function. We can partition similarly to the surface Green's function the S-matrix (the same way we did in (3.6)):

$$\mathbf{S} =: \begin{pmatrix} \mathbf{S}_{LL} & \mathbf{S}_{LR} \\ \mathbf{S}_{RL} & \mathbf{S}_{RR} \end{pmatrix} \equiv \begin{pmatrix} \mathbf{r} & \mathbf{t}' \\ \mathbf{t} & \mathbf{r}' \end{pmatrix} . \tag{3.46}$$

With these definitions we can express the S-matrix as:

$$(\mathbf{S}_{\beta\alpha})_{qp} = \langle \tilde{-}_q |_\beta \, \mathbf{g}^E_{\beta\alpha} \mathbf{V}_\alpha - \delta_{\beta\alpha} \, |+_p\rangle_\alpha \sqrt{\frac{|v^\beta(k_q^-)|}{|v^\alpha(k_p^+)|}} , \tag{3.47}$$

where $\alpha, \beta \in L, R$ and p/q goes over the open channels in the α/β leads. In this formula we used the convention that the $|+\rangle$ states travel towards the scattering region, and $|-\rangle$ states travel from the scattering region. This simplifies the formula, but we have to be careful since, in the previous derivations the positive direction was the positive direction of the x axis. This formula is the so called generalised Fischer-Lee relation. This was originally proposed by Fischer and Lee [12]. A more detailed and up to date derivation can be found in [13]. If the left and right leads are the same, and we are only interested in $\mathbf{t}$ this relation simplifies to:

$$t_{qp} = \langle \tilde{-}_q | \, \mathbf{g}^E_{RL} \mathbf{V} \, |+_p\rangle \sqrt{\frac{|v(k_q^-)|}{|v(k_p^+)|}} . \tag{3.48}$$

With this the transmission function can be calculated using (3.8).

3.6 Conductivity of two terminal setup

To summarize the things in this chapter we give a step by step algorithm to calculate the conductivity of a two terminal system. The Hamiltonian of the lead is (2.22) the Hamiltonian of the scattering region is constructed as explained in section 2.3.3. First we decimate the Hamiltonian of the leads as in (3.22), then we solve the (3.12) generalised eigenvalue problem. After that we calculate the surface Green's functions of the leads (3.31). After this we solve the surface Dyson equation (3.44). With the surface Green's function we calculate the transmission

amplitudes using (3.48). With this we calculate the transmission function as in (3.8). Finally we substitute this in the Landauer formula (3.3) and compute the conductance.

4 Scaling theory

In this chapter the basics of disordered electron systems, and the scaling theory of localization will be discussed. For further readings on this topic see [14], [15]. This topic is very broad and there are still many open questions so in this chapter we want only to highlight the most important concepts that we will study in section 5.4 numerically.

4.1 Scaling theory of localization

We saw in the previous chapter that the natural unit of the conductance is $G_o = 2e^2/h$. It is useful to define the dimensionless conductance as:

$$g := \frac{G}{G_o} \ . \tag{4.1}$$

We consider a disordered conductor, which is macroscopically homogeneous. Let's take a d dimensional hypercube of linear dimension L from this conductor. The conductance of this block is $g(L)$. The one-parameter scaling theory is based on the assumption that the dimensionless conductance alone determines the conduction behaviour of the system. This means that the conductance of hypercube of size L (where L is much larger than the mean free path) can be used to calculate the conductance of a hypercube of linear size $2L$ as:

$$g(2L) = f(g(L)) \ . \tag{4.2}$$

This means that no microscopic parameters are needed (such as the mean free path). This assumption can be extended to hypercubes with size $\alpha \cdot L$, where:

$$g(\alpha L) = f(g(L), \alpha) \ . \tag{4.3}$$

Let's define the scaling function (β) as the logarithmic derivative of g over L:

$$\beta := \frac{\mathrm{d}\log g(L)}{\mathrm{d}\log L} \ . \tag{4.4}$$

If (4.3) holds it can be shown that β can be expressed as a function of only g since:

$$\begin{aligned}\frac{\mathrm{d}\log(g(L))}{\mathrm{d}\log L} &= \frac{L}{g}\frac{\mathrm{d}g(L)}{\mathrm{d}L} = \frac{L}{g}\left.\frac{\mathrm{d}g(\alpha L)}{\mathrm{d}L}\right|_{\alpha=1} \\ &= \frac{1}{g}\left.\frac{\mathrm{d}g(\alpha L)}{\mathrm{d}\alpha}\right|_{\alpha=1} = \frac{1}{g}\left.\frac{\mathrm{d}f(g,\alpha)}{\mathrm{d}\alpha}\right|_{\alpha=1} = \beta(g) \ .\end{aligned} \tag{4.5}$$

The scaling function can be used to extrapolate a system to the thermodynamic limit. If $\beta(g) > 0$ the system scales toward higher conductances and if β remains positive for higher g values the system becomes a conductor in the thermodynamical limit. If $\beta(g) < 0$ the system scales towards lower conductances, so if β remains negative for lower conductances the system becomes an insulator in the thermodynamical limit. If $\beta(g) = 0$ we have a fixpoint, depending on the derivative of $\beta(g)$ it can be stable or unstable. If $\mathrm{d}\beta(g)/\mathrm{d}g > 0$ the fixpoint is unstable, and in the other case it is stable. If the fixpoint is stable it means that the system will scale toward a constant conductance. If the fixpoint is unstable the system will either scale toward a conductor or an insulator depending on the initial conductance.

4.2 Data collapse

If we assume that for different disorder strength the scaling function of the system is the same we get a very strong constraint on the $g(L)$ curves. At a given disorder strength we get a curve on the $\log g - \log L$ graph. Let's take two different disorder strength and call the corresponding curves $\log(g_1(\log L))$ and $\log(g_2(\log L))$. But since the logarithmic derivative can be expressed as a function of g at every $\log(g)$ value the derivative of the functions must be equal. This means that only a constant shift (c) can be the difference between the two functions so:

$$\log(g_2(\log L)) = \log(g_1(\log L + c)) \ . \tag{4.6}$$

This translates to the following without the logarithms:

$$g_2(L) = g_1(c \cdot L) \ . \tag{4.7}$$

This means that it is possible to rescale the length using a function dependent on the disorder strength (ε_d):

$$L^* = g(\varepsilon_d) \cdot L \ , \tag{4.8}$$

with which the g(L) curves of different disorder collapse to the same curve. This works well if we are far from the fixpoints, where $\beta(g) = 0$. Near a fixpoint after the collapse there should be three curves (one increasing, one decreasing and a constant line). In the case of an unstable fixpoint the three curves should diverge for bigger systems. In the case of a stable fixpoint the three curves should converge for bigger systems.

4.3 Classical theory of one parameter scaling

The theory presented here was introduced by Anderson [16]. This works well for quasi-free electrons, but has many important features that can be used for other systems as well.

For very high conductance $g \gg 1$ with many open channels one expects the Ohm's law to hold for the conductance. Thus the system can be described with a scale independent conductivity σ and the conductance can be calculated as:

$$G(L) = \sigma L^{d-2} \ . \tag{4.9}$$

this means that the scaling function is:

$$\beta(g) = d - 2 \ . \tag{4.10}$$

On the other hand when the conductance is very small (at very strong disorder) the Anderson localization [9] occurs. With this the conductance of the system will be exponentially small:

$$g(L) \propto \mathrm{e}^{-L/\xi} \ , \tag{4.11}$$

where ξ is the localization length. In this regime the β function is the following:

$$\beta(g) = \frac{\mathrm{d}}{\mathrm{d}\log L}\left(-\frac{L}{\xi} + const.\right) = -\frac{L}{\xi} = \log g + const. \tag{4.12}$$

Between the two asymptotic behaviour the easiest interpolation is the continuous monotonic one. This was the assumption made by Anderson, which is not true for every system as we will see later. We can see the schematic shape of the $\beta(g)$ function as showed by Anderson on figure 4.1.

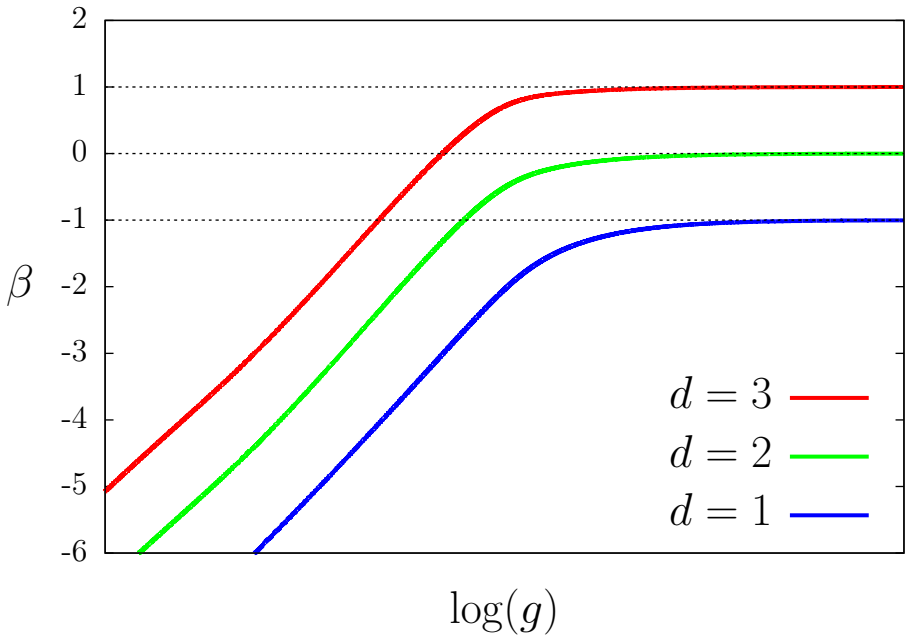

Figure 4.1: A sketch of the scaling function for different dimensions d as predicted by [16].

There are many consequences to this theory. In three dimensions we see that the scaling function is positive for high conductances and negative for low conductances. So there is a g_c critical conductance where there is an unstable fixpoint. This gives rise to the so called Anderson metal-insulator transition.

We see that in two and one dimension the β-function is always negative. Meaning that for a sufficiently large sample the system will be an insulator.

4.4 Scaling theory in two dimensions

The picture explained above is only valid for certain systems. Mostly systems where there are quasi-free electrons. The most important difference in our case is that the systems in two dimensions don't necessarily have an always negative β function. This means that it is possible to have metallic behaviour and also it is possible to have a metal-insulator transition in two dimension. This statement is supported by experimental result [17], theoretical [18] and numerical [19], [20], [7] calculations.

In systems from the symplectic symmetry class (time reversal symmetry, but no spin rotation symmetry) the scaling theory is still an open question. In the case of the Ando model in [20] they found that the scaling function has a fixpoint and the system shows a metal-insulator transition. In the case of graphene which also has symplectic symmetry results show that there is no transition and it has an always positive scaling function [7]. This is also supported by the arguments of [18].

5 Numerical Results

5.1 Numerical method

5.1.1 Setup

The studied system is an infinite strip of Lieb lattice. We can see the system on figure 5.1. In this work we will concentrate on the boundary conditions (b) and (c) from figure 2.6.

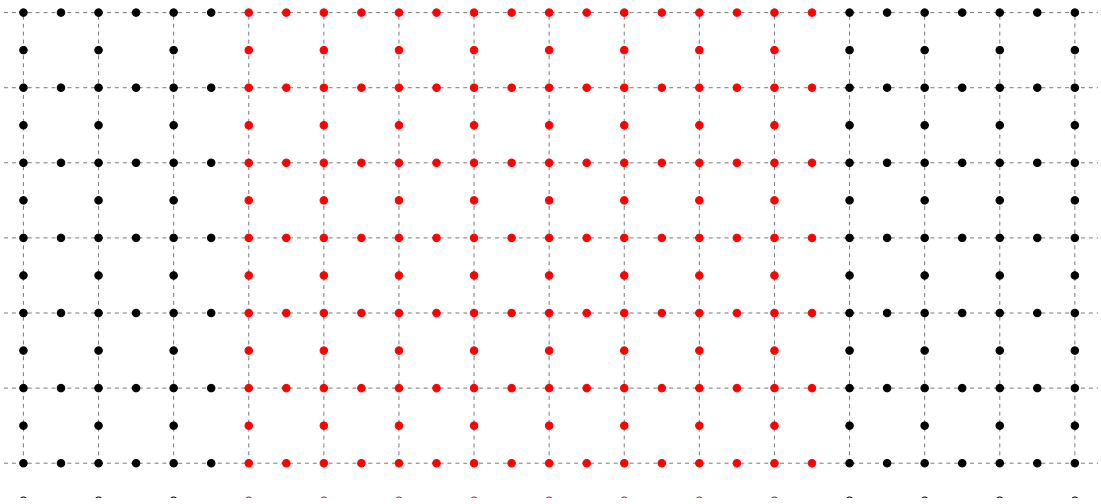

Figure 5.1: The studied Lieb lattice system with *closed* boundary condition. The black sites are the leads, the red sites are the scattering region. The dimension of the scattering region on this example is $W = 6$ and $L = 8$.

The Hamiltonian of the system can be constructed as explained in section 2.3. The part shown in black are the leads. They have $\varepsilon_\ell = -1.5$ on-site potential. At $E_F = 0$ Fermi energy they act as a good conductor with many open channels. The middle part in red is the scattering region. The width of the scattering region is W and the length is L. W and L are whole numbers representing the number of unit cells in the given direction.

The i-th site in the scattering region has on-site potential as described in section 2.3.3:

$$\varepsilon_i = \varepsilon_i^s + V_0 \ , \tag{5.1}$$

where ε^s is a random number from a uniform distribution in $[-\varepsilon_d, \varepsilon_d]$, with the constraint that $\sum_i \varepsilon_i^s = 0$. There is no disorder in the hopping parameters they are $\gamma = 1$ for every nearest neighbor.

5.1.2 EQuUs

For the numerical calculations the EQuUs program developed by the Eötvös Quantum Transport Group was used. The program is open source and can be downloaded from [21], also many informations can be found about the usage and implemented algorithms on this website.

I will give a brief introduction to the program and what can it be used for. For a deeper description see the website. EQuUs is written in MATLAB, it has many implemented routines to effectively carry out transport calculations using the Landauer Büttiker formalism. The program can also be used to treat superconductivity and magnetic field as well.

EQuUs can be used to calculate the steps explained in section 3.6. One has to define the Hamiltonian and with the implemented algorithms it is possible to carry out those steps.

We saw previously the structure of the Hamiltonian (see figure 2.9). The most upfront thing is that it is mostly empty. So for memory reasons it is useful to save only the nonzero elements in a sparse format. On top of that EQuUs uses the Intel MKL PARDISO package [22]. With the PARDISO package it is possible to calculate individual elements of the inverse of a sparse matrix. This in our case is very useful since we have sparse matrices, and we are only interested in the Green's function on the edge of the leads. We can read about the algorithm in [23]. This is a very important feature in EQuUs and it is crucial for the calculation of large systems.

5.1.3 NIIF HPC

The calculations were done on the Debrecen3-Phi supercomputer. This computer can be found at the University of Debrecen. The supercomputer is part of the NIIF Program (Nemzeti Információs Infrastruktúra Fejlesztési Program). The NIIF HPC (high performance computing) provide a lot of HPC resources to academic and research purposes (see [24] for more details).

The nodes which were used for the transport calculations are equipped with the so called Intel® Xeon Phi™ Coprocessor 7120P. This contains 61 cores with 4 threads each totaling 244 threads and it can be used for high performance calculations. The matrix inversion (needed in the Dyson equation) was done on these cards using the PARDISO package. This gave the possibility to collect data in a much higher rate on larger systems.

5.2 Conductance of pure system

In this section the pure Lieb lattice will be discussed. This is the case when $\varepsilon_d = 0$. The possible parameters are the size of the system L, the aspect ratio W/L and the V_0 potential.

First the $V_0 = 0$ case will be studied. From many calculations done on different sizes and aspect ratios the result we got was the following. For the *hanging* boundary condition, where there is a gap in the system we got $g = 0$ for every run. This can be understood since there is a gap the only available states are the states in the flat band. And even though there are many of these states $(W \cdot L)$ they have 0 group velocity, thus the carry no current. In the case of the *closed* boundary condition where there is no gap we get a constant $g = 1$ for every size and aspect ratio. This is a very unusal behaviour and it is caused by the gapless band.

A very important result for the case of graphene was the minimal conductivity [25]

5.3 Conductance with disorder

In this section we study the effects of disorder on the conductance. In practice we start using the ε_d parameter too. The studied disorders will be in the range $[0, 1]$, with the strongest disorder being equal to the hopping parameter. Since

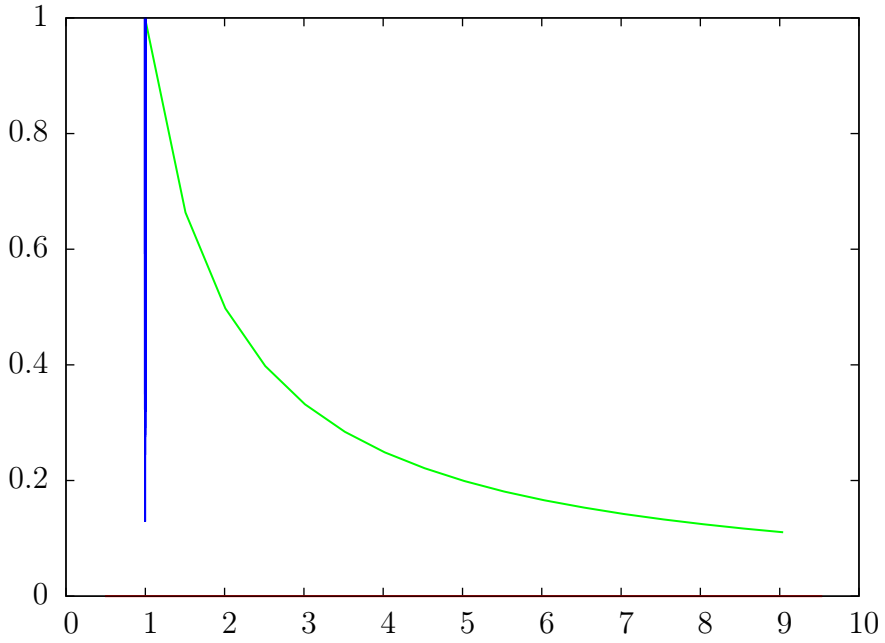

Figure 5.2: Conductivity aspectratio

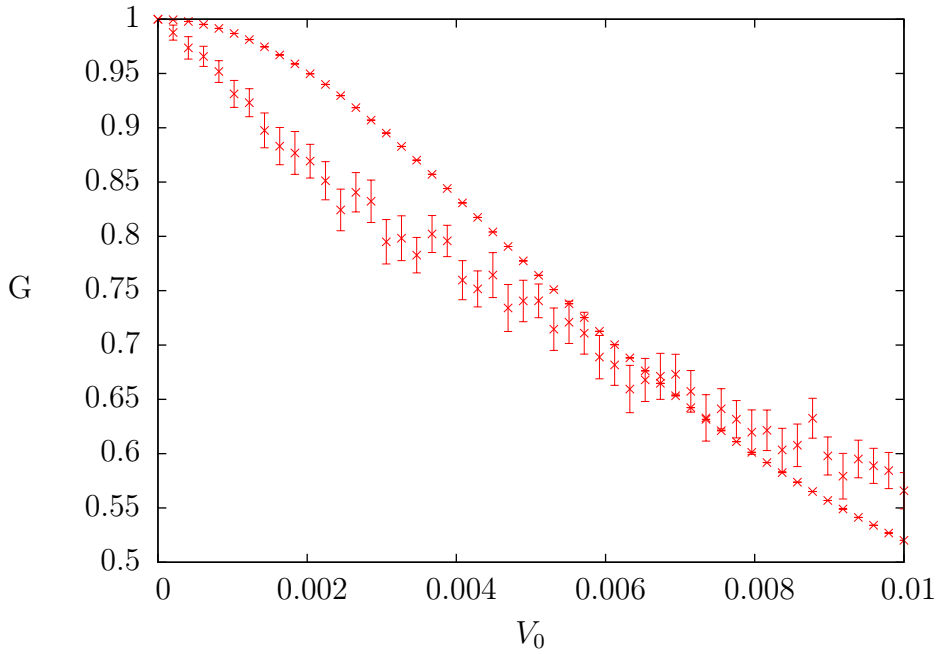

Figure 5.3: Gate

the disorder is taken from a random distribution, we need to do multiple calculations for the same parameters. This demands a lot of numerical calculations and computational time. For this reason it is convenient to reduce our parameter set and fix some of the parameters. Since we are expecially interested in the effects

of the flat band

Let's look first at the distribution of conductances using a fixed system size and fixed disorder.

n 0.01 és 0.1 s 0.01 és 0.1 s 1 n 0.001 s 0.05 50 100

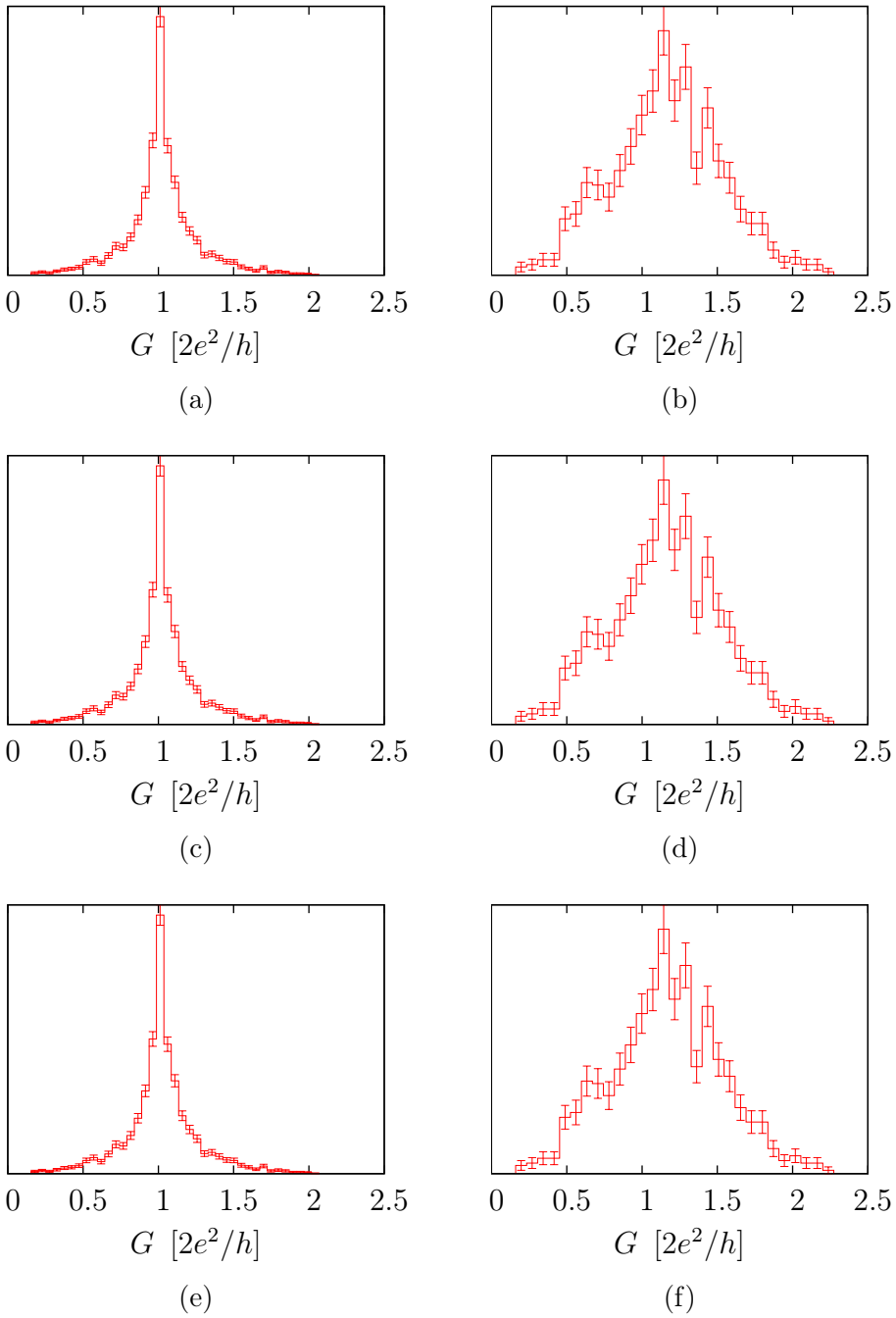

Figure 5.4: Dist 1

t probe

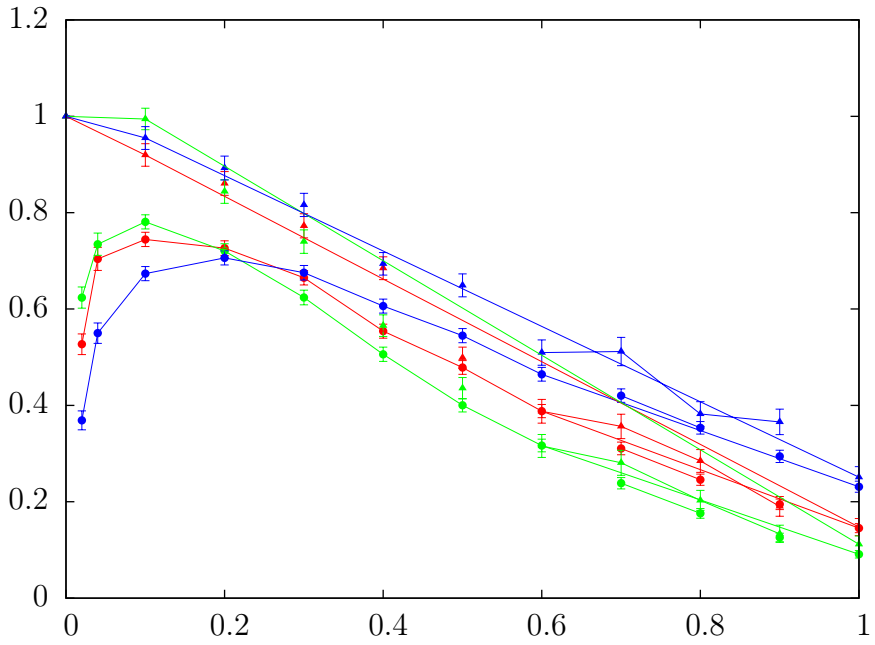

Figure 5.5: dis scaling

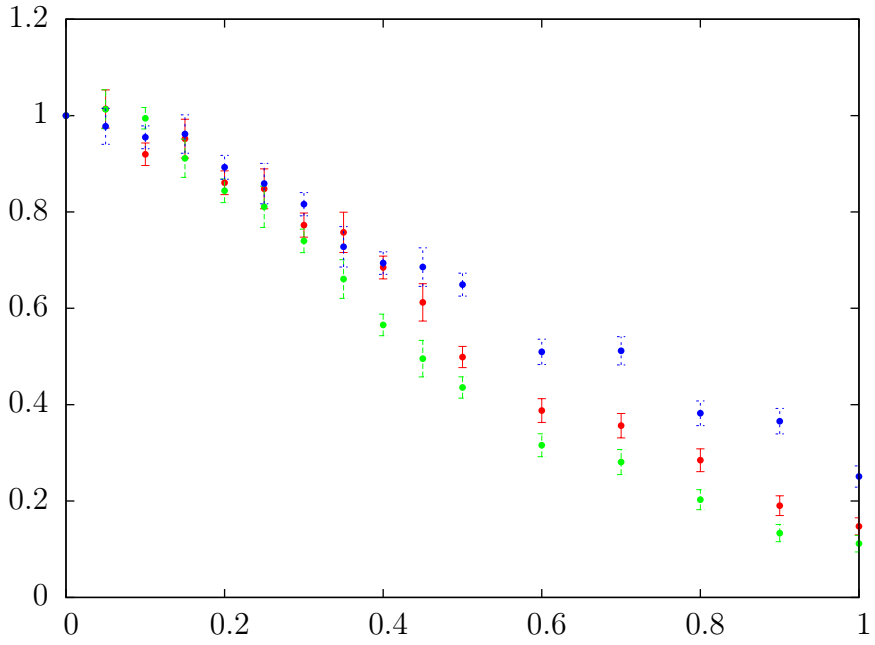

Figure 5.6: dis scaling

5.4 Scaling

To study the scaling properties of the Lieb lattice we need to evaluate the average conductance for the same ε_d at different system size L of the same aspect ratio.

Again we will only use square systems, so the aspect ratio will be one.

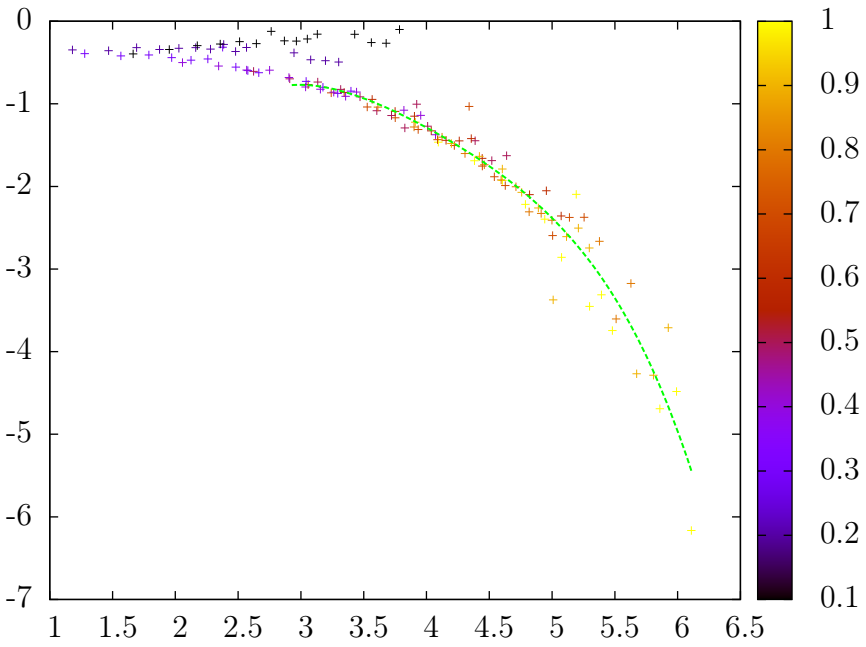

Figure 5.7: collapse

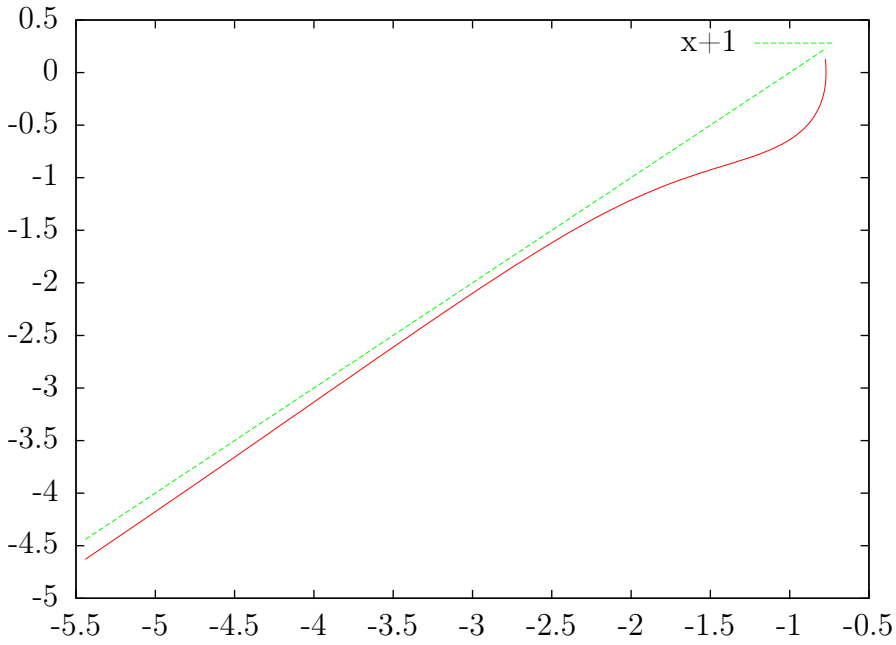

Figure 5.8: mybeta

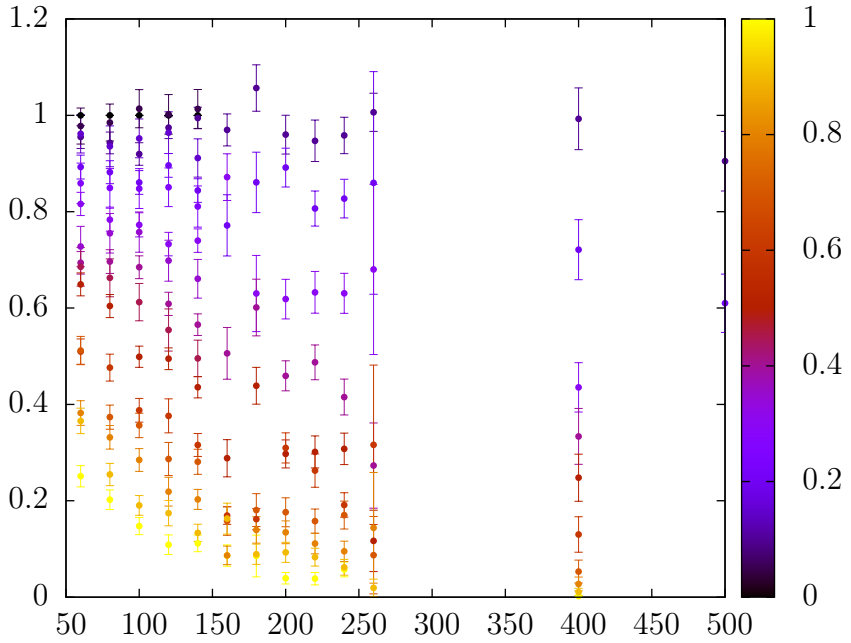

Figure 5.9: full scaling

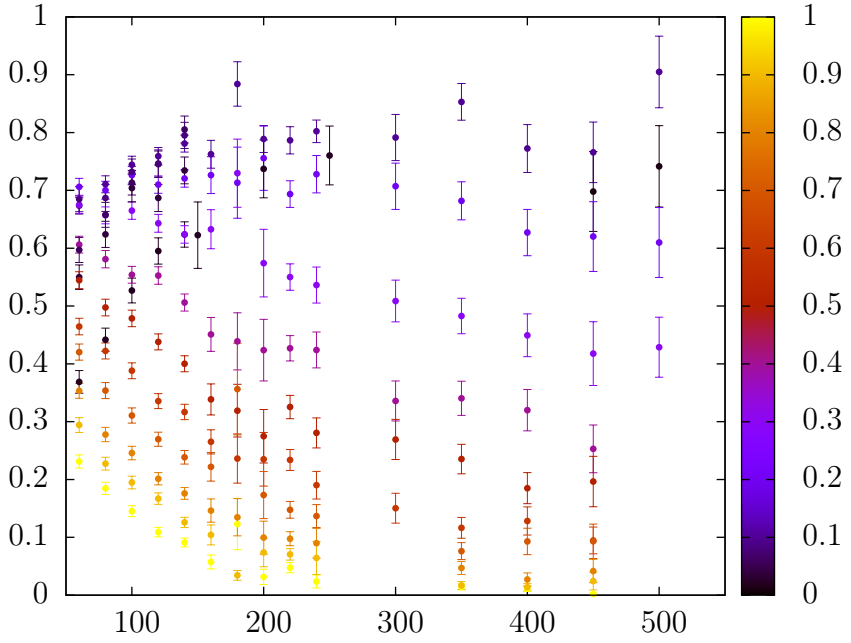

Figure 5.10: full scaling

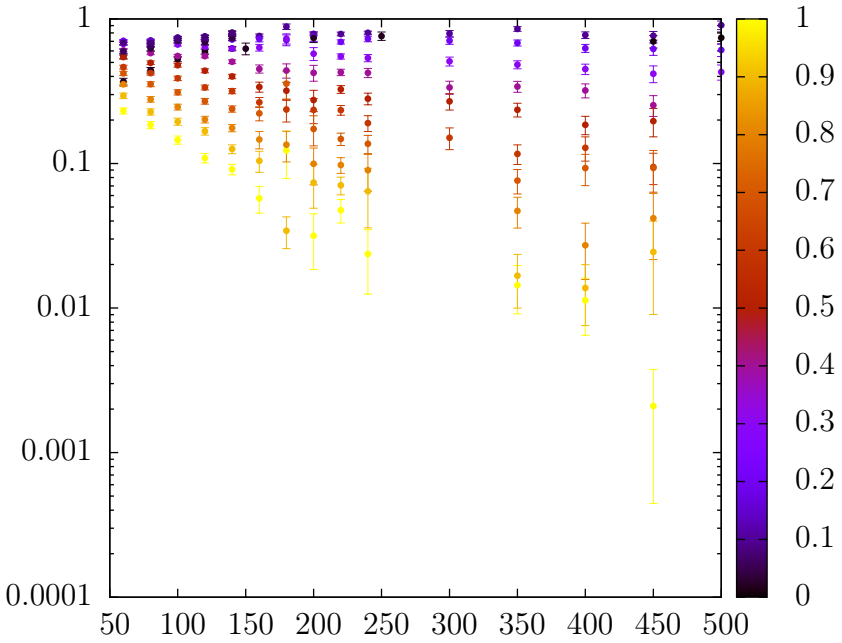

Figure 5.11: full scaling

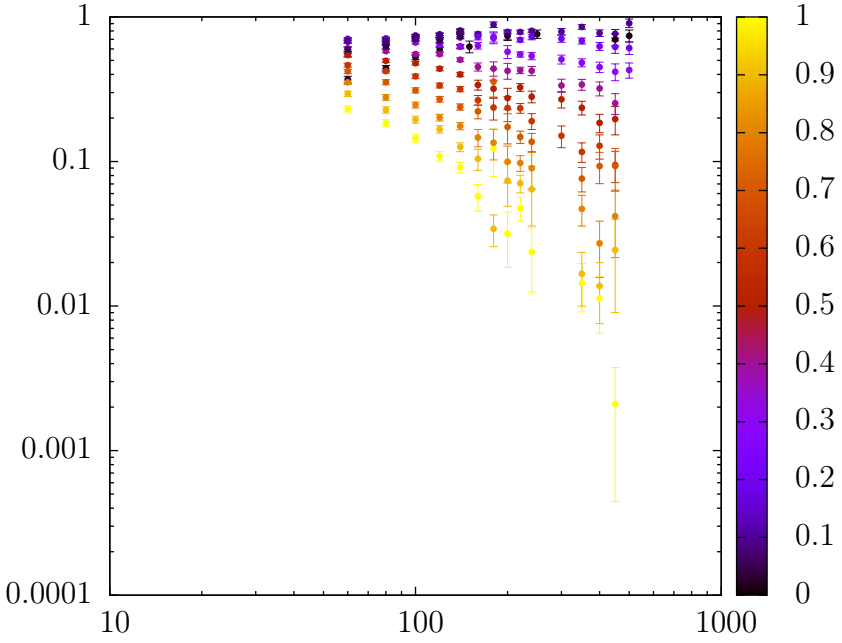

Figure 5.12: full scaling

6 Summary

<sum.tex>

6.1 Outlook

Acknowledgement

Appendix A

TB model of multiband systems

Let $a_\ell^{(i\sigma)}$ be the annihilation operator of the ℓ-th Wannier state at the i-th unit cell centered at $\mathbf{R}_i^\ell$ with spin σ. Let $w_l(\mathbf{r}-\mathbf{R}_i^\ell)$ be the wavefunction of the state created with $a_\ell^{(i\sigma)\dagger}$. The ℓ index can be used to describe multiple atoms in the same unit cell or different atomic orbitals too. In the framework of tight binding model we assume the Wannier states to be orthogonal (we neglect the overlap). We only consider states where the on site potential is zero. By having general on site potentials only the diagonal part of the Hamiltonian would change, so to get more transparent formulas we don't use any on site potential. The hopping parameters from the m-th state of the j-th unit cell to the ℓ-th state of the i-th unit cell are denoted with $\gamma_{ij}^{\ell m}$. We expect that the hopping parameter will be small between distant site-s, but we don't only allow nearest neighbor hoppings. All in all the second quantized Hamiltonian of an arbitrary tight binding system has the following form:

$$H = -\sum_{i,j,\sigma}\sum_{\ell,m}\gamma_{ij}^{\ell m}a_\ell^{(i\sigma)\dagger}a_m^{(j\sigma)} \ . \tag{A.1}$$

Applying Bloch's theorem we know that the Hamiltonian will be diagonal in the quasimomentum ($\mathbf{k}$). In systems were there are multiple atoms in a unit cell the Bloch representation is not unique [8]. For practical purposes the following representation will be used for the creation/annihilation operators of Bloch states:

$$a_\ell^{(\mathbf{k}\sigma)} = \frac{1}{\sqrt{N}}\sum_i \exp\bigl(-i\mathbf{k}\mathbf{R}_i^\ell\bigr)a_\ell^{(i\sigma)} \ . \tag{A.2}$$

The normalization is chosen so to assure the normalization of the Bloch states created with the creation operators from the vacuum. The inverse relations have

the following form:

$$a_\ell^{(i\sigma)} = \frac{1}{\sqrt{N}} \sum_{\mathbf{k}} \exp\big(i\mathbf{k}\mathbf{R}_i^\ell\big) a_\ell^{(\mathbf{k}\sigma)} \ . \tag{A.3}$$

Substituting these in the Hamiltonian:

$$\begin{aligned} H &= -\frac{1}{N} \sum_{i,j,\sigma} \sum_{\ell,m} \sum_{\mathbf{k},\mathbf{k}'} \gamma_{ij}^{\ell m} \exp\big(-i\mathbf{k}\mathbf{R}_i^\ell\big) \exp\big(i\mathbf{k}'\mathbf{R}_j^m\big) a_\ell^{(\mathbf{k}\sigma)\dagger} a_m^{(\mathbf{k}'\sigma)} \\ &= \sum_{\ell,m,\sigma} \sum_{\mathbf{k},\mathbf{k}'} a_\ell^{(\mathbf{k}\sigma)\dagger} a_m^{(\mathbf{k}'\sigma)} \sum_{i,j} -\frac{1}{N} \gamma_{ij}^{\ell m} \exp\big(-i\mathbf{k}\mathbf{R}_i^\ell\big) \exp\big(i\mathbf{k}'\mathbf{R}_j^m\big) \ . \end{aligned} \tag{A.4}$$

First we calculate the last part:

$$\begin{aligned} H_{\ell m}(\mathbf{k},\mathbf{k}') &:= -\frac{1}{N} \sum_{i,j} \gamma_{ij}^{\ell m} \exp\big(-i\mathbf{k}\mathbf{R}_i^\ell\big) \exp\big(i\mathbf{k}'\mathbf{R}_j^m\big) \\ &= -\frac{1}{N} \sum_i \exp\big(-i(\mathbf{k}-\mathbf{k}')\mathbf{R}_i^\ell\big) \sum_j \gamma_{ij}^{\ell m} \exp\big(i\mathbf{k}'\delta\mathbf{R}_{ji}^{m\ell}\big) \ , \end{aligned} \tag{A.5}$$

where $\delta\mathbf{R}_{ji}^{m\ell} = \mathbf{R}_j^m - \mathbf{R}_i^\ell$. Since we have a periodical system, the right sum is actually independent of i. We can think of it as a variable shift for every i, which doesn't alter the sum. For simplicity $i = 0$ will be chosen there. Knowing this the sum over i can be evaluated using $\sum_i \exp\big(-i(\mathbf{k}-\mathbf{k}')\mathbf{R}_i^\ell\big) = N\delta_{\mathbf{k}\mathbf{k}'}$:

$$H_{\ell m}(\mathbf{k},\mathbf{k}') = -\delta_{\mathbf{k},\mathbf{k}'} \sum_j \gamma_{0j}^{\ell m} \exp\big(i\mathbf{k}\delta\mathbf{R}_{j0}^{m\ell}\big) \ . \tag{A.6}$$

Going back to the full Hamiltonian our results simplifies to:

$$\begin{aligned} H &= \sum_{\ell,m,\sigma} \sum_{\mathbf{k}} a_\ell^{(\mathbf{k}\sigma)\dagger} a_m^{(\mathbf{k}\sigma)} H_{\ell m}(\mathbf{k}) \ , \\ H_{\ell m}(\mathbf{k}) &= \sum_j -\gamma_{0j}^{\ell m} \exp\big(i\mathbf{k}\delta\mathbf{R}_{j0}^{m\ell}\big) \ . \end{aligned} \tag{A.7}$$

Defining the Hamiltonian matrix ($\mathbf{H}(\mathbf{k})_{\ell m} = H_{\ell m}(\mathbf{k})$), and the vector of annihilation operators ($(\mathbf{a}_{\mathbf{k}\sigma})_\ell = \mathbf{a}_\ell^{(\mathbf{k}\sigma)}$) the Hamiltonian has the following form:

$$H = \sum_{\mathbf{k}\sigma} \mathbf{a}_{\mathbf{k}\sigma}^\dagger \mathbf{H}(\mathbf{k}) \mathbf{a}_{\mathbf{k}'\sigma} \ . \tag{A.8}$$

For calculating the dispersion relation all we need to do is solve the eigenvalue problem of $\mathbf{H}(\mathbf{k})$.

Appendix B

Decimation

In this appendix we show how can we eliminate certain sites by creating an energy dependent effective Hamiltonian. The advantage of this process is that we keep the eigenvalue spectrum unaffected while we reduce the size of the Hamiltonian. The process is especially useful for treating the singular $\mathbf{H}_1$ problem explained in section 3.2.1. Let's take an arbitrary $\mathbf{H}$ Hamiltonian matrix. The eigenvalue problem of $\mathbf{H}$ is:

$$\mathbf{H}\mathbf{\Psi} = E\mathbf{\Psi} \ . \tag{B.1}$$

First the case of decimating one site will be shown. If we want to get rid of the k-th site (where k is one of the indices of the $\mathbf{\Psi}$ vector) we can do the following. The eigenvalue problem for the k-th site looks like:

$$\sum_j H_{kj}\Psi_j = E\Psi_k \ . \tag{B.2}$$

We can separate Ψ_k on the left side as:

$$\sum_{j\neq k} H_{kj}\Psi_j + H_{kk}\Psi_k = E\Psi_k \ . \tag{B.3}$$

We can use this equation to express Ψ_k as:

$$\Psi_k = \sum_{j\neq k} \frac{H_{kj}\Psi_j}{E - H_{kk}} \ . \tag{B.4}$$

The eigenvalue problem for every other site is:

$$\sum_{j\neq k} H_{ij}\Psi_j + H_{ik}\Psi_k = E\Psi_i \quad i \neq k \ . \tag{B.5}$$

Now we can substitute (B.4) and get:

$$\sum_{j\neq k} H_{ij}\Psi_j + \sum_{j\neq k} H_{ik}\frac{H_{kj}\Psi_j}{E - H_{kk}} = E\Psi_i \quad i \neq k \ . \tag{B.6}$$

By defining the decimated Hamiltonian and decimated vector as:

$$\tilde{H}_{ij}(E) := H_{ij} + \frac{H_{ik}H_{kj}}{E - H_{kk}} \qquad \tilde{\Psi}_i := \Psi_i \qquad i,j \neq k \ , \tag{B.7}$$

the eigenvalue problem will be:

$$\tilde{\mathbf{H}}(E)\tilde{\mathbf{\Psi}} = E\tilde{\mathbf{\Psi}} \ . \tag{B.8}$$

As we can see this is now a smaller eigenvalue problem, but since the decimated Hamiltonian is energy dependent, it will be an implicit equation for E. By solving this we will end up we the original amount of eigenvalues. Similarly we can derive the decimated Hamiltonian if we want to get rid of a whole block. Let's say we want to eliminate the indices $k_0 < k < k_n$. We define $\mathbf{k} \equiv (k_0, ..., k)$. With this (B.3) becomes:

$$\sum_{j\notin\mathbf{k}} H_{\mathbf{k}j}\Psi_j + \sum_{j\in\mathbf{k}} H_{\mathbf{k}j}\Psi_j = E\Psi_{\mathbf{k}} \ , \tag{B.9}$$

where a single vector index means a vector with indices ranging through the indices in the vector. Again we can express $\Psi_{\mathbf{k}}$ as:

$$\Psi_{\mathbf{k}} = \sum_{j\notin\mathbf{k}} (E\cdot I_{\mathbf{kk}} - H_{\mathbf{kk}})^{-1} H_{\mathbf{k}j}\Psi_j \ , \tag{B.10}$$

Now similarly as (B.11) we get:

$$\sum_{j\notin\mathbf{k}} H_{ij}\Psi_j + \sum_{j\neq\mathbf{k}} H_{i\mathbf{k}}(E\cdot I_{\mathbf{kk}} - H_{\mathbf{kk}})^{-1} H_{\mathbf{k}j}\Psi_j = E\Psi_i \quad i \notin \mathbf{k} \ . \tag{B.11}$$

As we can see the decimated Hamiltonian can be calculated as:

$$\tilde{H}_{ij}(E) := H_{ij} + H_{i\mathbf{k}}(E\cdot I_{\mathbf{kk}} - H_{\mathbf{kk}})^{-1} H_{\mathbf{k}j} \qquad \tilde{\Psi}_i := \Psi_i \qquad i,j \notin \mathbf{k} \ , \tag{B.12}$$

Bibliography

[1] K. S. Novoselov, A. K. Geim, S. V. Morozov, D. Jiang, Y. Zhang, S. V. Dubonos, I. V. Grigorieva, and A. A. Firsov, "Electric field effect in atomically thin carbon films," *Science*, vol. 306, no. 5696, pp. 666–669, 2004.

[2] G. van Miert and C. M. Smith, "Dirac cones beyond the honeycomb lattice: A symmetry-based approach," *Phys. Rev. B*, vol. 93, p. 035401, Jan 2016.

[3] E. H. Lieb, "Two theorems on the hubbard model," *Phys. Rev. Lett.*, vol. 62, pp. 1201–1204, Mar 1989.

[4] S. Sanvito, C. J. Lambert, J. H. Jefferson, and A. M. Bratkovsky, "General green's-function formalism for transport calculations with spd hamiltonians and giant magnetoresistance in co- and ni-based magnetic multilayers," *Phys. Rev. B*, vol. 59, pp. 11936–11948, May 1999.

[5] I. Rungger and S. Sanvito, "Algorithm for the construction of self-energies for electronic transport calculations based on singularity elimination and singular value decomposition," *Phys. Rev. B*, vol. 78, p. 035407, Jul 2008.

[6] R. Landauer, "Spatial variation of currents and fields due to localized scatterers in metallic conduction," *IBM Journal of Research and Development*, vol. 1, pp. 223–231, July 1957.

[7] J. H. Bardarson, J. Tworzydło, P. W. Brouwer, and C. W. J. Beenakker, "One-parameter scaling at the dirac point in graphene," *Phys. Rev. Lett.*, vol. 99, p. 106801, Sep 2007.

[8] C. Bena and G. Montambaux, "Remarks on the tight-binding model of graphene," *New Journal of Physics*, vol. 11, no. 9, 2009.

[9] P. W. Anderson, "Absence of diffusion in certain random lattices," *Phys. Rev.*, vol. 109, pp. 1492–1505, Mar 1958.

[10] S. Datta, *Electronic transport in mesoscopic systems*. Cambridge studies in semiconductor physics and microelectronic engineering 3, Cambridge University Press, 1995.

[11] Y. T. a. Haruo Yanai, Kei Takeuchi, *Projection matrices, generalized inverse matrices, and singular value decomposition*. Statistics for Social and Behavioral Sciences, Springer-Verlag New York, 1 ed., 2011.

[12] D. S. Fisher and P. A. Lee, "Relation between conductivity and transmission matrix," *Phys. Rev. B*, vol. 23, pp. 6851–6854, Jun 1981.

[13] S. Sanvito, *Giant magnetoresistance and quantum transport in magnetic hybrid nanostructures*. PhD thesis, University of Lancaster, 2000.

[14] P. A. Lee and T. V. Ramakrishnan, "Disordered electronic systems," *Rev. Mod. Phys.*, vol. 57, pp. 287–337, Apr 1985.

[15] J. Rammer, *Quantum transport theory*. Frontiers in physics 99, Perseus Books, illustrated edition ed., 1998.

[16] E. Abrahams, P. W. Anderson, D. C. Licciardello, and T. V. Ramakrishnan, "Scaling theory of localization: Absence of quantum diffusion in two dimensions," *Phys. Rev. Lett.*, vol. 42, pp. 673–676, Mar 1979.

[17] V. M. Pudalov, "The metal–insulator transition in a two-dimensional system at zero magnetic field," *Physics-Uspekhi*, vol. 41, no. 2, p. 211, 1998.

[18] K. Nomura, M. Koshino, and S. Ryu, "Topological delocalization of two-dimensional massless dirac fermions," *Phys. Rev. Lett.*, vol. 99, p. 146806, Oct 2007.

[19] Y. Asada, K. Slevin, and T. Ohtsuki, "Numerical estimation of the β function in two-dimensional systems with spin-orbit coupling," *Phys. Rev. B*, vol. 70, p. 035115, Jul 2004.

[20] P. Markoš and L. Schweitzer, "Critical regime of two-dimensional ando model: relation between critical conductance and fractal dimension of electronic eigenstates," *Journal of Physics A: Mathematical and General*, vol. 39, no. 13, p. 3221, 2006.

[21] "Equus website," http://eqt.elte.hu.

[22] "Intel mkl pardiso," software.intel.com/en-us/node/470282.

[23] A. Kuzmin, M. Luisier, and O. Schenk, *Fast Methods for Computing Selected Elements of the Green's Function in Massively Parallel Nanoelectronic Device Simulations*, pp. 533–544. Berlin, Heidelberg: Springer Berlin Heidelberg, 2013.

[24] "Niif website," hpc.niif.hu/.

[25] J. Tworzydło, B. Trauzettel, M. Titov, A. Rycerz, and C. W. J. Beenakker, "Sub-poissonian shot noise in graphene," *Phys. Rev. Lett.*, vol. 96, p. 246802, Jun 2006.